# An Investigation into the Use of Stereophotogrammetry for the Analysis of Craniofacial Dysmorphology in Schizophrenia




**Michael Cousins**

**Division of Biomedical Engineering**

**University of Cape Town**

**A thesis submitted for the degree of**

*Master of Science*

**June 2015**

## DECLARATION

An Investigation into the Use of Stereophotogrammetry for the Analysis of Craniofacial Dysmorphology in Schizophrenia

I, Michael Cousins, hereby declare that:

1) This thesis with the above title is my own unaided work, and that apart from the normal guidance from my supervisor, I have received no assistance except as stated below.

2) Except where indicated to the contrary, neither the substance nor any part of this thesis with the above title has been submitted in the past, or is being , or is to be submitted for a degree in this university or any other university.

This thesis has been presented by myself and is being submitted for examination for the degree of Master of Science in Medicine in Biomedical Engineering at the University of Cape Town

Signed by candidate

Signature of Author

04 May 2015

---

Date

*For my wife, Charissa, who went through the trials and tribulations of this project as much as I did.*

# ACKNOWLEDGEMENTS

First and foremost, I would like to thank my supervisor, Prof Tania Douglas, for bearing with me for the lengthy duration of my project and for always being available when I needed her.

A special mention must be made of Dr Tinashe Mutsvangwa, who took me under his wing and showed me everything I needed to know in order to tackle this project, and even taking the time to answer my questions all the way from France. Later, he went on to co-supervise this project for which I cannot thank him enough.

I'd also like to thank everyone at Valkenberg Hospital and the UCT Psychiatry Department: Drs Henk Temmingh and Goodman Sibeko and Prof. Dan Stein, and especially Dr Fleur Howells. This project would not have happened without all your help with the patient recruitment and data collection.

# ABSTRACT

Studies of craniofacial dysmorphology in schizophrenia, carried out since the 1960s, have reported minor physical anomalies in those with schizophrenia, prominently in the craniofacial region. Indirect methods, most notably 3D laser imaging, have been used previously for investigating craniofacial dysmorphology in schizophrenia. This project aimed to investigate the ability of a stereophotogrammetry system to detect craniofacial dysmorphology in individuals diagnosed with schizophrenia. Furthermore, observed dysmorphology was characterised and compared with that found in previous studies.

Three-dimensional craniofacial landmark coordinates were obtained from images collected using a bespoke design stereophotogrammetry system. The system includes a camera rig and a calibration rig. On the camera rig is mounted three digital single-lens reflex cameras hardwired to a trigger for simultaneous image capture. The calibration rig consists of a frame with strategically positioned retro-reflective calibration markers of known 3D orientation.

The precision and reliability of the stereophotogrammetry system was tested using a human subject. Measurements were taken using the system and directly using callipers by two operators on two separate occasions. Intra- and inter-operator precision and inter-modality reliability were calculated and scored. All intra- and inter-operator precision scores were at least below a 7% error, and considered “good”. Inter-modality reliability scores had at least a “good” score in 72% of all measurements. Excluding one soft landmark and one landmark with small measurement value, all inter-modality reliability scores were at least “good”.

The study cohort consisted of 17 African (8 control, 9 schizophrenia) and 13 Caucasian (8 control, 5 schizophrenia) males. A set of 18 landmarks focused about the eyes, nose, mouth and chin was identified for each subject and collated in 3D coordinate space. Geometric morphometric analysis – particularly generalised Procrustes analysis and principal component analysis - was carried out on these landmark sets. Discriminant Function Analysis was applied to identify discriminating features in the data set, and classification techniques, aided by feature selection, were applied to separate affected and control subjects.

In the African cohort, the results showed wider inward slanting (cat-like) eyes, a wider upturned nose and narrower downturned mouth. In the Caucasian cohort, narrower and wide set eyes, a narrower downturned nose with anteriorly displaced alare, a wider downturned mouth and posteriorly set chin were shown. The Caucasian cohort demonstrates similar dysmorphology as described in the literature. Published data for the African cohort is lacking. The nearest mean and k-nearest neighbour classifiers had the highest accuracy in the African and Caucasian groups respectively, with 71% and 77% correct classification.

The efficacy of the stereophotogrammetry system introduced in this study has been shown, with craniofacial dysmorphology in schizophrenia successfully detected. Further studies with larger cohorts are recommended to attempt improved classification accuracy, but a platform now exists to pursue dysmorphology studies in other psychoses, such as bipolar disorder.

## CONTENTS

# LIST OF FIGURES

# LIST OF TABLES

# NOMENCLATURE

| | |
|---|---|
| $b$ | discriminant coefficient for feature $n$ |
| $g(\mathbf{x})$ | Bayes general classifier |
| $J$ | feature selection criterion function |
| $k$ | dimensionality |
| $L$ | discriminating function |
| $n$ | number of features |
| $N$ | number of shapes |
| $p(\mathbf{x}\|\omega_i)$ | conditional density |
| $P(\omega_i)$ | prior probability |
| $PC(r)$ | principal component $r$ |
| $S(\mathbf{x})$ | centroid size of shape vector $\mathbf{x}$ |
| $s_i^P$ | Procrustes shape coordinate |
| $s_i^{PR}$ | Procrustes residual |
| $\mathbf{x}$ | shape vector |
| $\bar{\mathbf{x}}$ | Procrustes mean |
| $\bar{x}, \bar{y}$ | centroid coordinates |
| $x, y, z$ | 3D coordinate system |
| $\gamma_r$ | direction of variance |
| $\lambda_r$ | variance expressed by principal component $r$ |
| $\omega$ | class label |

# 1. Introduction

Craniofacial dysmorphology has been investigated in psychosis because of the intimate relationship between cerebral and craniofacial morphogenesis during foetal development, which suggests that interruption of cerebral development can manifest as craniofacial dysmorphology. Such is the case with Down's syndrome (Hennessy, Kinsella, & Waddington, 2002) and foetal alcohol syndrome (Douglas & Mutsvangwa, 2010; Mutsvangwa & Douglas, 2007).

Minor physical anomalies in patients with schizophrenia have been well documented (Green, Satz, Gaier, Ganzell, & Kharabi, 1989; Guy, Majorski, Wallace, & Guy, 1983; Lohr & Flynn, 1993; Waldrop, Pedersen, & Bell, 1968). In these studies, anomalies were given scores based on their severity using a scale or derivative thereof developed by Waldrop et al. (1968) which assessed features of the head, eyes, ears, mouth, hands and feet. Later studies used direct anthropometry, using callipers, measuring tapes and protractors to take physical measurements (Fakhroddin, Ahmad, & Imran, 2014; Lane et al., 1997; Lin et al., 2014). Such studies found prominent dysmorphology in the craniofacial region, however there seems to be a lack of consistency in the dysmorphology identified.

Several methods of indirect anthropometry have been successfully employed to detect craniofacial dysmorphology. Amongst the more established methods are photogrammetry, for surface features, and cephalometry, for skeletal features (Allanson, 1997; Douglas, 2004). Photogrammetry entails measurement from photographs. The concept of photogrammetry has been expanded to stereophotogrammetry, incorporating the capture and analysis of multiple images from different perspectives to provide three-dimensional information (Douglas, 2004). 3D laser scanners have also been employed successfully in craniofacial anthropometry (Hennessy, Baldwin, Browne, Kinsella, & Waddington, 2007, 2010; Hennessy et al., 2002). A recent study using 3D laser scanning successfully identified significant craniofacial dysmorphology in bipolar disorder similar to but less pronounced than those found schizophrenia (Hennessy et al., 2010).

The primary advantage of stereophotogrammetry over 3D laser scanning is that it provides a cheaper alternative, while still providing 3D facial data. Therefore stereophotogrammetry could prove to be a more cost effective tool for craniofacial assessment than 3D laser scanning.

Craniofacial dysmorphology has been characterised successfully in children with foetal alcohol syndrome (FAS) and foetal alcohol spectrum disorders (FASD) at the University of Cape Town using stereophotogrammetry (Douglas & Mutsvangwa, 2010; Meintjes et al., 2002; Mutsvangwa & Douglas, 2007). Consequently, a sound methodology for the use of stereophotogrammetry in

craniofacial morphometric analysis has been established which is applied in this project. This study draws from the experience gained in these previous studies when applying stereophotogrammetry to the detection of facial dysmorphology in schizophrenia.

## 1.1 Objectives

This study aimed to employ stereophotogrammetry for craniofacial morphometric analysis of patients with schizophrenia in comparison with healthy subjects. It sought to determine whether an analysis system using landmark-based stereophotogrammetry and geometric morphometrics is able to identify craniofacial dysmorphology in schizophrenia in agreement with the findings of previous studies, for Caucasian and African participants.

The objectives were to:

- Validate the stereophotogrammetric equipment as a measurement tool for the facial features shown in the literature to be relevant to schizophrenia.
- Apply geometric morphomteric methods to facial landmark data obtained using the stereophotogrammetry system in order to identify morphological differences between control subjects and those diagnosed with schizophrenia.
- Use classification tools to distinguish between affected and control subjects.

## 1.2 Ethics Approval

This study is approved by the Faculty of Health Sciences Human Ethics Committee of the University of Cape Town (UCT HSF HREC 078/2009).

## 1.3 Dissertation Overview

Chapter 2 provides a review of literature pertinent to this study. Included in the literature reviewed are studies on schizophrenia, neurodevelopmental hypotheses and craniofacial anthropometric studies, as well as anthropometric and statistical shape analysis methods and their application in facial anthropometric studies.

Chapter 3 provides the theory for the geometric morphometric techniques employed in this study, including shape manipulation for analysis, methods for dimensionality reduction while retaining important discriminating features and methods for using these features to discriminate between groups.

Chapter 4 details the stereophotogrammetric system used in this project, including its different components and software used for craniofacial analysis.

Chapter 5 describes the methodology and implementation of tests to evaluate the precision and reliability of the stereophotogrammetry system. The results of these tests are also described in this chapter.

Chapter 6 outlines the methodology used in this study, describing participant selection and screening, and image acquisition and processing prior to analysis. The method of analysis is described including the application of the different software for the processing of the images, landmark identification and statistical shape analysis.

Chapter 7 analyses the results from the geometric morphometric analysis of the study cohort, seeking to identify any similarities or dissimilarities between the groups.

Chapter 8 reflects on the implementation of the stereophotogrammetric system in the identification of craniofacial dysmorphology in schizophrenia in comparison with previous findings in literature. Any limitations in the current study are discussed and recommendations for future modifications to the system and study structure are presented.

# 2. Review of Relevant Literature

The literature reviewed in this chapter includes work on the neurodevelopmental model of schizophrenia, introducing the concept of craniofacial dysmorphology. A review is provided of the development of different anthropometric methods, and their applications to distinguish sex and race and to identify craniofacial dysmorphology in schizophrenia. Finally, statistical shape analysis is reviewed including its use in craniofacial anthropometry.

## 2.1 Neurodevelopmental Model of Schizophrenia

Schizophrenia is described as a disorder characterised by hallucinations and delusions, lack of motivation and volition, reduced spontaneous speech, social withdrawal, alterations to memory, attention and executive function and depressive and manic (bipolar) moods (van Os & Kapur, 2009).

The neurodevelopmental model for schizophrenia is well defined, attributing a predisposition to schizophrenia to pre- and perinatal disturbances affecting development of certain portions of the brain.

Several studies describe correlations between developmental anomalies and schizophrenia. These include perinatal and early childhood developmental disturbances and environmental and genetic factors. Maternal illness, stress and malnutrition and obstetric complications have been linked to an increased risk of schizophrenia in the offspring (Murray & Lewis, 1987; van Os & Kapur, 2009; Waddington, Lane, Larkin, & O'Callaghan, 1999). Cognitive functioning and development were shown to be interrupted or inhibited in those who would later develop schizophrenia. Social and behavioural development is impaired, with schizophrenia patients said to have suffered from attention deficit, anxiety and depression in early years (Rapoport, Addington, Frangou, & Psych, 2005; van Os & Kapur, 2009). Waddington et al. (1999), Rapoport et al. (2005) and van Os & Kapur (2009) report susceptibility genes predisposing patients to schizophrenia. Waddington et al. (1999) highlight numerous studies that successfully identify minor physical anomalies present in the craniofacial region in patients with schizophrenia and furthermore the classification of a phenotype of frontonasal dysmorphology associated with schizophrenia. This classification enables researchers to isolate that period during pregnancy where insult occurs and to identify the period of cerebral morphogenesis that is disrupted. This in turn could aid in narrowing the definition of the neurodevelopmental model of schizophrenia, which is still quite broad (Rapoport et al., 2005).

## 2.2 Craniofacial Dysmorphology in Schizophrenia

Several early studies investigating craniofacial dysmorphology in schizophrenia employed the Waldrop scale, a scoring system assessing the presence and severity of different anatomical abnormalities (Waldrop et al., 1968), when investigating the minor physical anomalies in subjects with schizophrenia. A score is given for specific anomalies, including size and shape of the eyes, ears, mouth, hands and feet. The higher the score, the more severe the anomaly. One such study found a direct relationship between Waldrop score, and therefore minor physical anomalies, and the severity of the disorder in Caucasian adult males (Guy et al., 1983). Another study, on Caucasian adults, noted a high incidence of minor physical anomalies around the mouth. Additionally, the study also found a correlation between age of onset and more prevalent physical anomalies, suggesting a neurodevelopmental process involved with schizophrenia (Green et al., 1989).

Later studies used quantitative methods to assess craniofacial dysmorphology in schizophrenia patients. One such study chose dimensions of the eyes, ears, nose, mouth, hand and foot from a Caucasian group, while concurrently applying the Waldrop scale. The study revealed numerous minor physical anomalies, more so than the Waldrop scale, primarily in the craniofacial region. The group provided a phenotypic characterisation of this craniofacial dysmorphology, stating "an overall narrowing and elongation of the mid-facial and lower facial region with widening of the skull base and extensive anomalies of the mouth, ears and eyes" and attributed twelve dysmorphic features distinguishing schizophrenia (Lane et al., 1997). Another study carried out in Iran used direct anthropometric methods in tandem with the Waldrop scale (Fakhroddin et al., 2014). They reported increased coronal (tragion to tragion over the top of the head) and sagittal (glabella to opsithocranion over the top of the head) arc lengths and decreased overall head height.

The use of quantitative methods for assessing minor physical anomalies, as well as the neurodevelopmental hypothesis associated with schizophrenia, led to a vast increase in the number of studies investigating craniofacial dysmorphology in schizophrenia with little agreement on the characterisation of this dysmorphology. A meta-analysis of ultimately a select few studies that met inclusion criteria showed notable dysmorphology in the areas of the mouth, head, eye, foot, hand and ear. Minor physical anomalies were most prevalent around the mouth, but the meta-analysis concluded that no single region proved statistically more susceptible to dysmorphology (Weinberg, Jenkins, Marazita, & Maher, 2007).

Studies have sought to investigate sex-specific craniofacial differences in schizophrenia, particularly in the frontonasal region (Hennessy et al., 2004, 2007). The findings are detailed in Table 2.1.

| | Male | Female |
|---|---|---|
| Face | • Laterally broader<br>• Lengthened lower mid-facial height<br>• Shortened upper mid-facial height<br>• Posteriorly set nasion | • Laterally broader<br>• Lengthened lower mid-facial height<br>• Shortened upper mid-facial height<br>• Posteriorly set nasion<br>• Smaller and posteriorly set frontonasal process |
| Eyes | • Anteriorly and inferiorly set | • Wider and anteriorly and inferiorly set |
| Nose | • Posteriorly set subnasale<br>• Broader and down-turned | • Anteriorly set subnasale<br>• Narrower and up-turned |
| Mouth | • Narrower and posteriorly set | • Narrower and posteriorly and superiorly set |
| Mandible | • Chin narrower and posteriorly set<br>• Mandible wider postero-laterally | • Chin narrower and posteriorly and superiorly set<br>• Mandible wider postero-laterally |

**Table 2.1: Findings from investigations into sex-specific craniofacial dysmorphology associated with schizophrenia** (Hennessy et al., 2004, 2007).

A further study considered sex-specific differences in a predominantly African-American group (Compton, Brudno, Kryda, Bollini, & Walker, 2007). The Compton study found that female schizophrenia patients had greater mid-facial depths (right and left tragus – subnasale), smaller mid-facial height (nasion – subnasale) and greater lower facial height (subnasale – gnathion). Male schizophrenia patients showed lesser forehead (trichion – glabella) and lower face (subnasale – gnathion) heights.

## 2.3 Methods of Craniofacial Anthropometry

The techniques employed in craniofacial anthropometry can be divided into direct and indirect methods, each with their own advantages and disadvantages. All anthropometric methods share three components of examination: landmark location, measurement and evaluation against normative data (Farkas & Deutsch, 1996).

### 2.3.1 Direct Anthropometry

Direct anthropometry uses instruments including various callipers, tape measures and protractors to take linear and angular measurements of the head, face, eyes, nose, mouth and ears (Farkas, 1994). It offers measurement of areas which would be obscured by hair or pose or that would be distorted using indirect methods and allows the palpation of bony landmarks for easier measurement in some instances. Also, there is relatively low cost involved with direct anthropometry (Douglas & Mutsvangwa, 2010).

However, patient examination can be prolonged and the examiner requires a certain level of expertise to perform the measurements accurately. Acceptable data is heavily reliant on subject cooperation and the examination procedure (Farkas & Deutsch, 1996). No permanent record of the subject is obtained other than the measurement figures acquired during examination (Allanson, 1997). Contact of instruments with soft tissue may distort the facial surface and landmarks repeatedly used in different measurements need to be relocated with each measurement (Douglas, 2004). These factors greatly increase the risk of error. Certain measurements, such as those around the eye, can cause discomfort and anxiety in patients when done using direct anthropometry, and could lead to injury.

### 2.3.2 Indirect Anthropometry

Indirect methods of craniofacial anthropometry include photogrammetry, cephalometry and laser scanning. Indirect anthropometry requires a shorter interaction with the subject and no physical contact with the subject and is less dependent on subject compliance (Farkas & Deutsch, 1996).

Photogrammetry is the process of obtaining measurements from photographs of the object in question. The use of a single view may prove inadequate in the measurement of 3D space due to the 2D nature of photographs and so losing the aspect of depth. Stereophotogrammetry is the use of two or more cameras to extract 3D information of the object. The environment in which the images are captured must be controlled as poor lighting can negatively affect the image quality. Cephalometry carries the same principles as photogrammetry but uses X-ray images and has also been applied to obtain 2D and 3D information (Douglas, 2004). The principal disadvantage of cephalometry is the inability to identify soft-tissue landmarks (Allanson, 1997).

Stereophotogrammetry is used to facilitate the 3D reconstruction of the subject using multiple 2D images of the subject's craniofacial region captured by two or more digital cameras. In order for stereophotogrammetry to be successful, a coordinate system is required to which the position of the cameras can be described. With the camera orientation known, the 3D coordinates of a point occurring on two or more 2D images can be obtained relative to that same coordinate system. A calibration frame with known geometric properties can be positioned around a subject's head to aid in 3D reconstruction of the landmarks of the face (Douglas, 2004). Stereophotogrammetry has advantages over direct anthropometry due to the enhanced data analysis gained from statistical shape analysis methods, over single photogrammetry because of the inherent error of deriving measurements of a 3D form from a 2D image, and over 3D surface imaging because of cost considerations.

Three-dimensional laser scanning is often used in conjunction with a photogrammetric system. Either the photogrammetric system captures a narrow laser beam swept across the subject's face or a coded light pattern is cast onto the facial surface and the distortion of this pattern on the face is captured by the digital cameras (Douglas & Mutsvangwa, 2010). Alternatively, a structured or patterned laser light source is projected onto the subject surface while digital cameras capture the data (Majid, Chong, Ahmad, Setan, & Samsudin, 2005). Laser scanning offers high accuracy of data capture. Laser light projected onto a subject with darker complexion and onto hair does not reflect well and can hinder the capture process. Initially, scan times of several seconds were reported (Douglas, 2004; Majid et al., 2005), but later this time was reported to be as rapid as 0.6 seconds (Mutsvangwa, 2009). In comparison to photogrammetry however, which features instantaneous image capture, capture time using laser scanning is slower and could lead to a motion artefact compromising the image quality.

### 2.3.3 Comparison of Craniofacial Features between Gender and Ethnic Groups

Normative anthropometric data must be established prior to investigation of dysmorphology. For investigations with a cohort of different races, normative data must be found for each race. Additionally, sex- and race-specific craniofacial morphology highlights the necessity to discriminate between groups when carrying out any morphological study.

Gender-specific craniofacial morphometric studies have identified marked differences between the sexes. A study employing 3D laser scanning, landmark extraction and geometric morphometric analysis to investigate these differences, found that females have a wider and flatter face, the eyes are laterally and anterior set, while the nasion the positioned set. The nose is narrower, smaller and protrudes less. The lips are thicker and the upper lip and chin are both set posteriorly (Hennessy et al., 2002).

A comprehensive inter-ethnic anthropometric study was conducted, drawing 1470 participants from 25 countries from five regions worldwide: Europe, the Middle East, Asia, Africa and North America. The participants were pooled into four groups: Caucasian (13 countries), Middle Eastern (3 countries), Asian (5 countries) and African (4 countries) (Farkas et al., 2005). Using a direct anthropometric approach, a series of 14 linear and angular measurements were carried out: head and face (4 vertical, 2 horizontal), eye (3 horizontal), nose (1 vertical, 1 horizontal, 1 angular), mouth (1 horizontal) and ear (1 vertical) (Figure 2.1). North American Caucasian (NAC) data was used as a comparative reference.

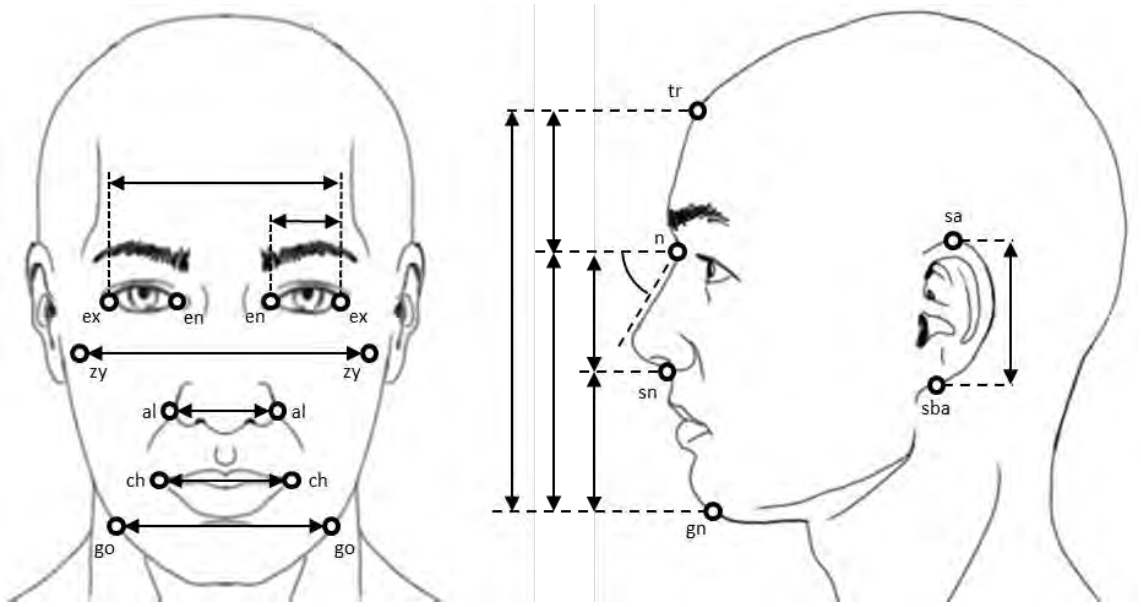


**Figure 2.1: The 14 craniofacial measurements. al, alare; ch, cheilion; en, endocanthion; ex, exocanthion; gn, gnathion; go, gonion; n, nasion; sa, superaurale; sba, subaurale; sn, subnasale; tr, trichion; zy, zygion** (Adapted from Farkas et al. (2005))**.**

The results from the study ranked scores for each measurement as either extremely or very significant, with each described as greater or less than the NAC data. The authors summarised their findings as follows. Generally, no significant differences were reported in oral or aural measurements in any ethnic groups. Amongst the Caucasian group, the facial width in males and mandibular widths in both sexes was greater than the NAC reference group. Additionally, the eye fissure length and biocular widths were greater, more so in males. Amongst the Middle Eastern group, no significant differences were reported in head and face measurements. Intercanthal and eye fissure dimensions were significantly greater than the NAC group, while the biocular length was significantly smaller. It was found that the nasal length was significantly greater in Middle Eastern females. Much like the Caucasian group, facial and mandibular dimensions were significantly greater in Asian males while only the mandibular width was greater in females. Mostly, intercanthal and biocular measurements were greater and eye fissure length smaller than the NAC group. The nose was in general wider in both sexes. In the African group, the head and facial measurements were similar to the NAC group. No significant difference was found for the intercanthal measurement and the biocular length was greater. The findings of the eye fissure length were inconclusive. The nasal measurements show a wider nose than the NAC group for both sexes in the African group.

The same research group conducted another inter-ethnic study comparing African-American and North American Caucasians (Farkas, Katic, & Forrest, 2007). Using direct anthropometric techniques,

51 linear, angular and circumferential measurements of the head, face, eyes, nose, mouth and ears were taken from 100 African-American participants and compared to previously established North American Caucasian measurements. The authors reported significant differences in all regions in males, with the most extensive and highly significant differences occurring eyes and nose. All horizontal measurements and inclinations of the eye region were greater in the African-American group. Vertical measurements were smaller. Of the nasal region measurements, all vertical were smaller and horizontal greater in the African-American group. Amongst the female population, extensive significant differences were found in all regions. All vertical measurements of the face were greater in the African-American group. Horizontal and angular dimensions of the oral region were all greater. Regarding the nasal region, the vertical measurements were all smaller and horizontal measurements greater in among African-Americans. All measurements, vertical and horizontal, were greater in the oral region. In the ear region, the vertical measurements were smaller, but the angular measurements greater in the African-American group. Very few significant differences were identified in horizontal measurements of the head and face in both sexes.

Specific to the black South African population, 200 participants of Bantu heritage were photographed to attempt the identification of distinguishing features (Roelofse, Steyn, & Becker, 2008). Measurements between standard biometric landmarks of the face, eyes, nose and mouth were taken directly from the photographs. The study reported what they determined common features within Bantu-speaking South Africans such as oval, inverted trapezoidal and rectangular facial shapes. Common features included a downward-turned nose, shallow or absent philtrum, V-shaped upper lip notch, absent nasiolabial fold and intermediate nasal bridge.

A review of inter-ethnic studies sought to determine the variability between races (European, African, East Asian, South Asian and Native American) and which features best discriminate between them (Fang, Clapham, & Chung, 2011). Measurements were classified into five categories: least variable, less variable intermediate, intermediate, more variable intermediate, most variable. Table 2.2 illustrates the conclusions from this review.

| Least variable | Less variable intermediate | Intermediate | More variable intermediate | Most variable |
|---|---|---|---|---|
| zy – zy<br>ex – ex | go – go<br>sa – sba<br>en – ex | n – sn<br>ch – ch<br>sn – gn<br>al - al | en – en | tr – n |

**Table 2.2: Inter-ethnic variation. al, alare; ch, cheilion; en , endocanthion; ex, exocanthion; gn, gnathion; go, gonion; n, nasion; sa, superaurale; sba, subaurale; tr, trichion; zy, zygion** (Fang et al., 2011)**.**

The review concludes that the forehead height contributes the most inter-ethnic variability while the midface and biocular widths offer the least inter-ethnic variability.

## 2.4 Statistical Shape Analysis

Statistical shape analysis is the examination of a set of shapes to describe geometric properties within a population or to compare different groups to identify traits discriminating one group from another. It has been used extensively in studies implementing indirect anthropometric methods such as 3D laser scanning. Most commonly, the method of statistical shape analysis used in these studies is geometric morphometrics.

Geometric morphometrics is method of statistical shape analysis which retains the geometry of the landmark configurations, that is, preserves the relationships between object features, throughout measurement, allowing the results to be displayed as actual shapes (Mitteroecker & Gunz, 2009). This is superior to traditional morphometrics, which is based on arbitrarily collected distances, ratios and angles without considering the spatial relationship of the landmark configuration (Rohlf, 1999). Generally, geometric morphometrics is used to determine if covariance between shapes exists, that is, a correlation between change in shape, and to describe that covariance (Bookstein, 1991).

Shape can be considered the geometric information remaining once location, scale and rotational effects are removed from an object, while form is considered as the shape of an object taking into consideration its size, that is, the scaling artefact is not removed (Mitteroecker & Gunz, 2009; Stegmann & Gomez, 2002). Landmark coordinates can be described using Cartesian coordinates as loci with labels, to imply homology between forms (Bookstein, 1991). . Accordingly, a finite number of landmarks or point vectors $n$ can be used to describe shape in a finite number of planes $k$, such that the shape vector is mathematically represented as a $(k \times n)$ vector (Rohlf, 1999; Stegmann & Gomez, 2002). This is achieved through triangulation of the landmark coordinates from some common datum (Bookstein, 1991).

### 2.4.1 Geometric Morphometrics for Craniofacial Anthropometry

Several studies have employed varying geometric morphometric techniques for analysing craniofacial morphology, not only investigating dysmorphology on schizophrenia (Buckley et al., 2005; Compton et al., 2007; Hennessy et al., 2004, 2007; Lane et al., 1997), but also bipolar disorder (Hennessy et al., 2010), foetal alcohol syndrome (Meintjes et al., 2002; Mutsvangwa & Douglas, 2007; Mutsvangwa, Meintjes, Viljoen, & Douglas, 2010), autism (Aldridge et al., 2011; Obafemi-Ajayi et al., 2014) and Downs' syndrome (Zhao et al., 2013). Similar techniques have also been employed

to study non-disorder craniofacial morphologies, such as sexual dimorphism (Hennessy et al., 2002) and differences in regional or ethnic groups (Farkas et al., 2005, 2007; Hennessy & Stringer, 2002).

Hennessy & Stringer (2002) and Hennessy et al. (2004, 2007, 2010), when investigating craniofacial differences between different regional groups and in schizophrenia and bipolar disorder respectively, used 3D laser surface imaging to record craniofacial features. Geometric morphometric analysis was generally carried by initially testing for overall shape difference between groups using either Goodall's F test or Hotelling's $T^2$ test. Generalised Procrustes analysis (GPA) was carried out to produce Procrustes residuals, the distances between each shape and the mean shape following GPA. Principal component analysis (PCA) was employed to investigate shape variability between groups. Finally, a regression step (linear, multiple, discriminant function analysis) was carried out to identify those principal components (PCs) which best distinguish the two groups in question.

Generalised Procrustes analysis, principal component analysis, feature selection and classification techniques are discussed in further detail in Chapter 3 below.

Buckley et al. (2005), in their investigation into craniofacial dysmorphology in schizophrenia patients, used a 3D camera to capture multiple images of each subject to produce a 3D image of the craniofacial region. Analysis was carried out as per a previous study by the same authors (Buckley et al., 1999). Landmarks were manually identified and demarked on the digital images and the Procrustes mean and residuals were calculated. The between-group to within-group squared Procrustes distances ratio was used in a Goodall's F test to evaluate significance.

Three-dimensional cameras have been used in investigations into craniofacial dysmorphology in autism spectrum disorders (Aldridge et al., 2011; Obafemi-Ajayi et al., 2014). The first study used Euclidean Distance Matrix Analysis (EDMA), a linear-based morphometric method. EDMA calculates all possible distances between landmark pairs and produces a form matrix (FM) for each subject. Average FMs for each group are produced and compared, producing a form difference matrix (FDM). A non-parametric bootstrapping algorithm was then used to test significance. A PCA was also performed to group like shapes based on the landmarks and identify linear distances that influence group formation. The second study also employed similar linear-based morphometric methods (geodesic distance computation) and clustering analysis. Statistical comparisons were made through univariate one-way analysis of variance (ANOVA) and Student's *t* test.

Stereo-photogrammetry systems have been utilised in analysing craniofacial dysmorphology investigating foetal alcohol syndrome (Meintjes et al., 2002; Mutsvangwa & Douglas, 2007;

Mutsvangwa et al., 2010). The first study employed direct linear transform to convert the two-dimensional data from the individual images into three-dimensional data for analysis. Inter-landmark distances were measured and checked for statistical significance using a Student's *t* test. The second and third studies, much like those studies using 3D laser surface imaging, tested for overall shape difference between groups using GPA, Goodall's F test, PCA and discriminant function analysis (DFA), a linear classifier.

Studies employing direct anthropometric techniques have also carried out quantitative and statistical analysis on inter-landmark measurements (Compton et al., 2007; Farkas et al., 2005; Lane et al., 1997). The Compton and Lane studies investigated craniofacial dysmorphology in schizophrenia, while the third study investigated facial morphology between different ethnic groups. Both schizophrenia studies investigated between group comparisons using the Student's *t* test. Cluster analysis (Compton et al., 2007) and ANOVA (Lane et al., 1997) were then carried out to assess whether a combination of measurements could discriminate patients from controls. The ethnic study merely used standard deviations about a chosen control group to determine craniofacial differences between groups. Statistical significance was explored by calculating the p-value for each measurement.

## 2.5 Summary

The hypothesis that schizophrenia is a neurodevelopmental disorder is well supported, evidenced by multiple documented findings of physical anomalies present in those diagnosed with the disorder. These anomalies or dysmorphology have not yet unequivocally been defined; however this may be due to a lack of standardised measurement protocol. Recent studies, using 3D laser scanning technology, have proposed phenotypes in male and female Caucasian populations, detailing distinctions of the eyes, nose, mouth and face. Previous studies have commented on overall face and head size at best.

There is also very little reported on the shape variation in ethnic groups outside of Caucasian populations. Furthermore, it would appear that those that do investigate craniofacial dysmorphology in other populations have used direct anthropometric techniques.

There seems to be no evidence of investigations into craniofacial dysmorphology in schizophrenia using photogrammetry or stereophotogrammetry exclusively, that is, without structured light or laser. Such systems have been implemented successfully in the detection and characterisation of craniofacial dysmorphology in foetal alcohol syndrome.

Investigations using another anthropometric modality such as stereophotogrammetry could add support to the characterisation of a phenotype associated with schizophrenia, but only if comparable measurements are taken to those described in the literature. Additionally, the majority of studies seem to be carried out in developed countries with better access to technologies such as 3D laser scanning and in Caucasian populations. Stereophotogrammetry as described in this study could provide an alternative to 3D laser scanning, given the potential cost benefits. This could make image-based craniofacial dysmorphology research more accessible to the developing world and potentially initiate further research in other ethnicities.

# 3. Geometric Morphometrics: Theory

This chapter describes the geometric morphometric concepts applied in the project. These include: Procrustes superimposition, the normalisation of all shapes within a set so that their distance to a mean shape is minimised; principal component analysis, the determination of those shape features that display the greatest variation within the set; discriminant function analysis, the identification of those features of greatest variation that best discriminate between groups within the set; feature selection, a dimensionality reduction technique which creates subsets that best represent the original dataset; and classification, methods of assigning data into either predetermined or logical groups.

## 3.1 Procrustes Superimposition

Procrustes superimposition seeks to define the parameters describing the shapes of homologous landmark configurations (Mitteroecker & Gunz, 2009). It is a least-squares oriented approach involving four steps: centroid calculation, scaling, translational alignment and rotational alignment (Stegmann & Gomez, 2002). Translation aligns all shapes within the set to the same centroid, which is often positioned at the origin of the coordinate system. The centroid is calculated by determining the mean of the landmarks in each dimension.

$$(\bar{x}, \bar{y}) = \left( \frac{1}{n} \sum_{j=1}^{n} x_j , \frac{1}{n} \sum_{j=1}^{n} y_j \right)$$

where $n$ is the number of landmarks and $j = 1, \dots n$.

All landmark configurations are scaled to the same centroid size $S(\mathbf{x})$, defined as the root of the sum of the squared differences between the shape coordinates and the centroid.

$$S(\mathbf{x}) = \sum_{j=1}^{n} \sqrt{\left(x_j - \bar{x}\right)^2 + \left(y_j - \bar{y}\right)^2}$$

The centroid size is often set to unity for all shapes. Once centred and scaled, each shape is rotated about the centroid using the rotation matrix $\mathbf{VU^T}$ until the sum of the squared distances between homologous landmarks is minimised (Stegmann & Gomez, 2002).

$$\mathbf{VU^T} = \begin{bmatrix} \cos\theta & -\sin\theta \\ \sin\theta & \cos\theta \end{bmatrix}$$

Figure 3.1 illustrates Procrustes superimposition using two homologous shapes in two-dimensional space.

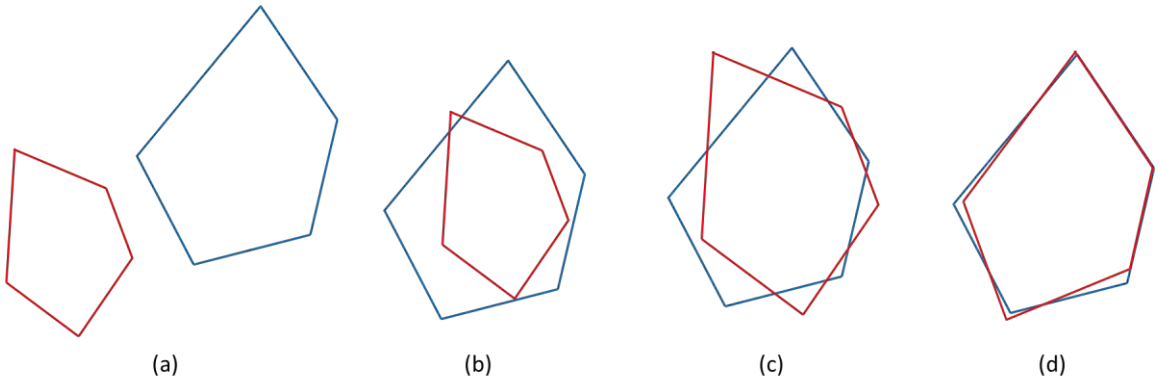


**Figure 3.1: Procrustes superimposition of two homologous shapes. (a) Raw landmarks, (b) translation to a common centroid, (c) scaling to the same unit centroid size, (d) rotation to minimise the Euclidean distance between corresponding landmarks** (adapted from Mitteroecker & Gunz (2009))**.**

When aligning a number of shapes, an iterative algorithm known as generalised Procrustes analysis is used, whereby all shapes are rotated to an arbitrary estimate. The resultant coordinates are averaged and realignment is carried out. This is repeated until convergence is achieved. To produce an initial estimate, the Procrustes mean $\bar{\mathbf{x}}$ is applied, which is simply the sum of all the shape vectors $\mathbf{x}_i$ divided by the number of shapes in the set.

$$\bar{\mathbf{x}} = \frac{1}{N}\sum_{i=1}^{N} \mathbf{x}_i$$

where $N$ is the number of shapes in the set and $i = 1, \ldots N$.

The resultant coordinates following alignment are known as Procrustes shape coordinates.

$$\left(s_{i_{jx}}^{P}, s_{i_{jy}}^{P}, s_{i_{jz}}^{P}\right)$$

The differences between each aligned shape and the mean are known as Procrustes residuals.

$$\left(s_{i_{jx}}^{PR}, s_{i_{jy}}^{PR}, s_{i_{jz}}^{PR}\right)$$

Figure 3.2 shows the result of Procrustes superimposition with the Procrustes mean shape (dots) about the centroid (*) and Procrustes shape coordinates (crosses) after superimposition and the resultant Procrustes residuals (dashed lines).

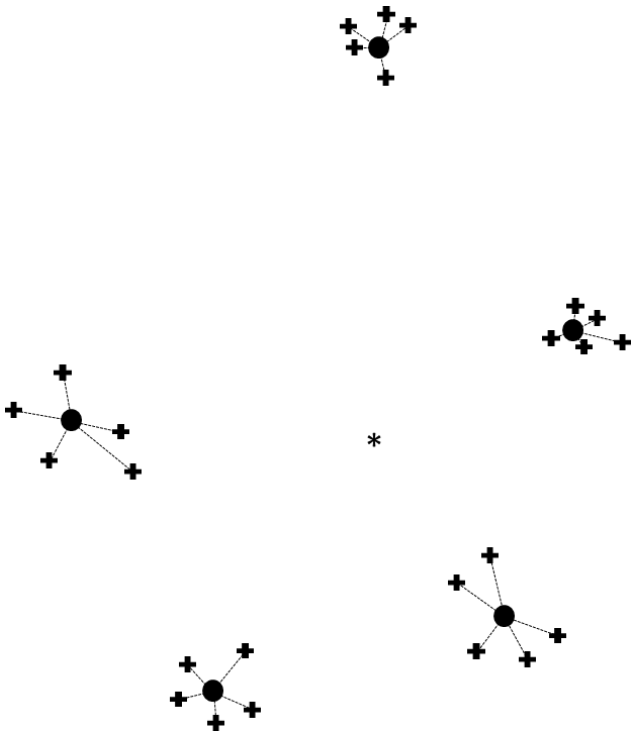

**Figure 3.2: Example of Procrustes superimposition with centroid (*), Procrustes means (dots), Procrustes shape coordinates (crosses) and Procrustes residuals (dashed lines) (adapted from** Bookstein (1991)**).**

The distance between two sets of Procrustes shape coordinates is known as Procrustes distance and describes the similarity or dissimilarity between the two landmark configurations. Both Procrustes residuals (Stegmann & Gomez, 2002) and Procrustes distance (Mitteroecker & Gunz, 2009) can be used in principal component analysis, a linear multivariate method, to assess shape variability.

The space occupied by the aligned shapes can be considered to be a subset of a non-Euclidean hyper-sphere. In order to carry out linear multivariate analysis, a Euclidean representation of the non-Euclidean shape vectors must be constructed. Tangent space projection modifies the shapes by projecting the shape vectors onto a hyper-plane tangential to the hyper-sphere, thus creating a linear representation of those shape vectors (Rohlf, 1999; Stegmann & Gomez, 2002), which can be considered a new set of shape variables (Klingenberg, 2011). When the shape variation is small enough, the Procrustes residuals can be used as a good approximation of the Procrustes tangent coordinates (Rohlf, 1999).

## 3.2 Principal Component Analysis

Principal component analysis (PCA) is utilised to examine the main features of shape variation within a sample (Klingenberg, 2011). It reduces the set of variables to those that best represent the variation in the data. The projection of the shape vectors onto this lower-dimensional space gives

rise to principal component scores. These scores allow for the assessment of group differences, group trends and outliers (Mitteroecker & Gunz, 2009).

PCA is carried out via eigen-decomposition of the covariance matrix of the shape set and is a rigid rotation of the data, preserving the Procrustes distance. Principal components are computed by calculating the eigenvectors and eigenvalues of the covariance matrix of the shape set. The covariance matrix $C$ is a set of covariance values, covariance $cov(X,Y)$ being the measure of the relationship between two dimensions within a shape set. A covariance matrix for a three-dimensional data set is shown below.

$$cov(X,Y,Z) = \frac{\sum_{i=1}^{n}(X_i - \bar{X})(Y_i - \bar{Y})(Z_i - \bar{Z})}{n-1}$$

where $X$ and $Y$ are the dimensions in question, $n$ the number of measurements in the set and $i = 1, \dots n$.

$$C = \begin{pmatrix} cov(x,x) & cov(x,y) & cov(x,z) \\ cov(y,x) & cov(y,y) & cov(y,z) \\ cov(z,x) & cov(z,y) & cov(z,z) \end{pmatrix}$$

The principal components can be considered to be these calculated eigenvectors, with the magnitude of the corresponding eigenvalues determining the statistical significance of each principal component. Being eigenvectors with corresponding eigenvalues, principal components have similar properties to eigenvectors. All principal components are orthogonal to each other and therefore statistically uncorrelated. Each component represents the variability in the sample, with the first principal component showing the largest variability and continuing in decreasing order. Finally, every principal component is a linear combination for the original variable (Halazonetis, 2004).

There are as many principal components as there are landmark coordinates, $(k \times n)$. Removing those principal components with little statistical significance (with smaller eigenvalues) reduces the dimension of the shape set, making statistical analysis simpler without compromising the integrity of the data (Smith, 2002).

Relating Procrustes superimposition and principal component analysis, principal components can be expressed using the Procrustes residuals. The $r^{th}$ principal component can be expressed as

$$PC(r) = \sum_{j}^{n} \left( \gamma_{r_{jx}} s_{jx}^{PR}, \gamma_{r_{jy}} s_{jy}^{PR}, \gamma_{r_{jz}} s_{jz}^{PR} \right)$$

where $\gamma_{r_{jx}}$, $\gamma_{r_{jy}}$ and $\gamma_{r_{jz}}$ describe the direction of variation in each Procrustes coordinate about the mean shape.

To visualise the shape variability represented by each principal component, the average shape can be distorted by manipulating coordinates according to the weight of each principal component. The $r^{th}$ principal component can be plotted using the following coordinates.

$$\left(\bar{\mathbf{x}}_{jx} + c\sqrt{\lambda_r \gamma_{r_{jx}}}, \bar{\mathbf{x}}_{jy} + c\sqrt{\lambda_r \gamma_{r_{jy}}}, \bar{\mathbf{x}}_{jz} + c\sqrt{\lambda_r \gamma_{r_{jz}}}\right)$$

where $\lambda_r$ is the variance expressed by the $r^{th}$ principal component and $c$ is a standard deviation about the mean shape, typically $-3 \leq c \leq 3$ (Mutsvangwa, 2006, 2009).

Using the above equations, the shape variability about the mean shape can be determined for each principal component. These equations were modified by Mutsvangwa (2006, 2009) for analysis of facial dysmorphology, from a previous study employing Procrustes superimposition and principal component analysis to explore tooth shape (Robinson, Blackwell, Stillman, & Brook, 2001).

Those principal components contributing most to shape variation are then subjected to feature analysis for classification of groups within the shape set.

### 3.3 Discriminant Function Analysis

Discriminant function analysis (DFA) is a data reduction technique used to make decisions about group membership based on the features within that dataset. It analyses whether a set of measurements (independent variables) can predict group membership (the dependent variable) by identifying which variables are the best discriminators between groups (Ramos & Rickard Liow, 2013).

DFA has two basic steps. The first is the F test (Wilks' lambda) which determines whether or not the discriminant model as a whole is significant. If the F test does show significance, then the individual independent variables are assessed to see which differ significantly. Those that prove significant can then be used to classify the dependent variables.

Classification of the dependent variables is achieved through a linear combination of the independent variables. This is known as the discriminating function and it maximises the differences between the dependent variables.

$$L = b_1 x_1 + b_2 x_2 + \cdots + b_n x_n + c$$

where $L$ is the discriminating function, $b_{1\text{-}n}$ are the discriminant coefficients, $x_{1\text{-}n}$ are the independent variables and $c$ is a constant.

DFA can be used to carry several tasks including the classification of cases into groups, testing theory by observing whether cases are classified as predicted, investigating difference between groups, identifying the most prudent means to distinguish between groups, determining the percentage variance within groups explained by the independent variables, and assessing the relative importance of the independent variables in classification of the dependent variables (Garson, 2012).

## 3.4 Classification

Classification provides a predictive model that initially explains the difference between objects of different classes by observing the features and measurements of these objects and then predicts the class of some unlabelled object (Webb & Copsey, 2011). To define a classifier it is first important to understand the concept of a mapping. A mapping is a transformation operating on a dataset, the dataset being a matrix of a number of objects and their features, memberships or some set of properties. Objects here are defined as vectors of *k*-dimensions with *n* features (feature values, (dis)similarities or class memberships). The space defined by the features is called feature space and objects are points or vectors in this space. A classifier is a specialised mapping that maps the objects in the dataset on class labels (Duin et al., 2007).

Classification is typically carried out by assigning a portion of the dataset to a training set. The class allocation of each object in this training set is known. The remainder of the dataset with no class allocation is then tested against this training set and, given the object features of this test set, the classifier attempts to separate this test set into the known classes. Training in this manner requires larger datasets due to the necessity of assigning a portion of this dataset for training.

The degree of success of each classifier can be tested, typically through probability of error. Probability of error tests the likelihood of misclassification for each classifier using the training and test sets (Duin et al., 2007).

For smaller datasets, it may not be viable to allocate a portion of the data to a training set as this may compromise the statistical power of the data. In this case, probability of error may not be an option. Instead, leave-one-out cross-validation can be used. This is a rolling method whereby a single object is set aside for testing against the remaining objects, which can be considered a training set. This is carried out for all available objects and the results averaged.

Untrained classification seeks to separate objects without prior training into logically established classes given the features of each object and their orientations with respect to one another. This is generally employed only when the classes of a dataset are unknown. Obviously in the case of untrained classification, error analysis as explained above cannot be carried out as there are no known classes to reference.

### 3.4.1 Linear and Higher Degree Polynomial Classifiers

A variety of classifiers have been defined. Linear and higher degree polynomial classifiers assign classes to objects through linear or higher degree polynomial combinations of the object features. Examples of linear and higher polynomial classifiers include Fisher's linear classifier, nearest mean classifier and logistic linear classifier.

#### 3.4.1.1 Fisher's Linear Classifier

Fisher's linear classifier seeks to find a linear combination of the variables that yields maximum separation between the two classes (Webb & Copsey, 2011). The criterion influencing the classifier is the ratio of between-class and within-class variances, that is, the relationship between the class means and their covariance matrices.

#### 3.4.1.2 Nearest Mean Classifier

The nearest mean classifier is applied by simply calculating the mean of each class and assigns objects according to their relative position to each class mean (van der Heijden, Duin, de Ridder, & Tax, 2005).

#### 3.4.1.3 Logistic Linear Classifier

The logistic linear classifier estimates maximum likelihood parameters using logistic regression, making assumptions about the log-likelihood ratios between classes (Webb & Copsey, 2011). While nonlinear optimisation is required to estimate these parameters, the discrimination step is still linear.

### 3.4.2 Normal Density Bayes Classifiers

Normal density based classifiers follow Bayesian decision theory, a cost-benefit exercise using prior probabilities between the various classification parameters by applying a likelihood ratio (Duda, Hart, & Stork, 2000). A general Bayes classifier designed to minimise error is expressed as:

$$g_i(\mathbf{x}) = \ln p(\mathbf{x}|\omega_i) + \ln P(\omega_i)$$

where $\omega$ is a class, $\mathbf{x}$ are features within the class, $p(\mathbf{x}|\omega_i)$ are the conditional densities (likelihood) and $P(\omega_i)$ are the prior probabilities.

Examples of normal density Bayes classifiers include linear and quadratic normal Bayes classifiers, both derived from the function above. In the linear case, it is assumed that the variance for all classes is considered equal, hence the covariance matrix is diagonal. This is not the case in the quadratic discriminant function (Duda et al., 2000).

The assumptions made in each function affect the first term of the general Bayes classifier function (the conditional densities) and ultimately affects the thresholds and the hyperspace defined for classification. The linear discriminant function describes decision surfaces of hyperplanes, subspaces one dimension lower than that of the dataset. Graphically, these are represented as straight lines. The quadratic discriminant function describes decision surfaces of hyperquadrics, conic subspaces of the original dataset. Graphically, these are represented of parabolic or higher order curves.

### 3.4.3 Nonlinear Classifiers

Nonlinear classifiers refer to those classifiers not considered linear or higher degree polynomial. Examples of nonlinear classifiers include support vector machines and k-nearest neighbour classifier.

#### 3.4.3.1 Support Vector Machines

Support vector machines map pattern vectors to a high-dimensional feature space where an optimal separating “maximal margin” hyperplane is defined (Webb & Copsey, 2011). Figure 3.3 illustrates the application of a support vector machine. Two distinct data sets are separated by hyperplane A. There are numerous arbitrary hyperplanes that will satisfactorily separate the data sets, as illustrated on the left. The support vector machine produces a hyperplane with a “maximal margin” which maximises the sum of the distances from the hyperplane to the closest object in each of the classes. This margin is two hyperplanes symmetrically positioned about the separating hyperplane, as shown on the right. In carrying out this operation, support vector machines maximise classifier performance and reduce classifier error.

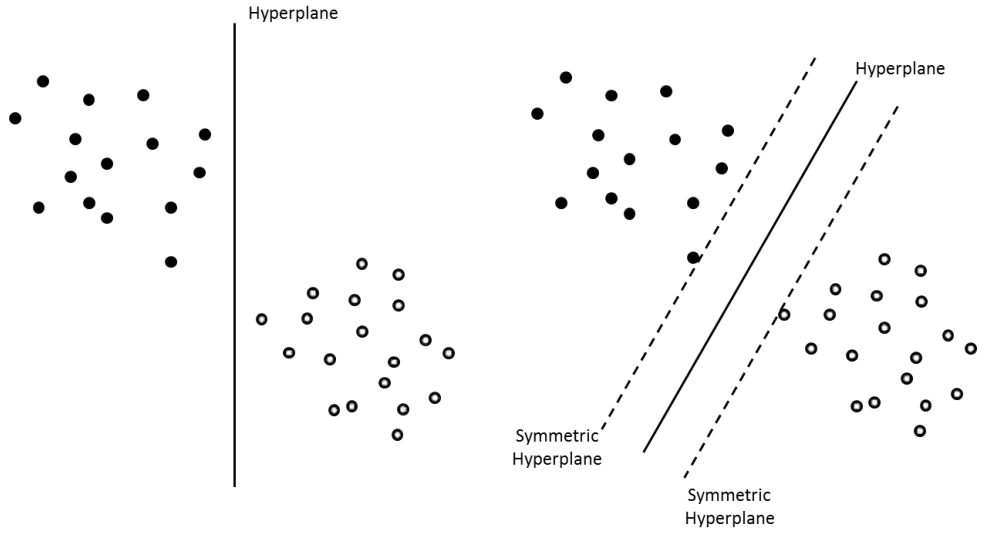


**Figure 3.3: Demonstration of support vector classification (right) versus arbitrary linear classification (left)** (adapted from Webb & Copsey (2011))**.**

### 3.4.3.2 k-Nearest Neighbour Classifier

$k$-nearest neighbour classifiers for classifying feature $\mathbf{x}$ into class $\omega$ determine the $k$ nearest training data vectors to $\mathbf{x}$ using some distance metric and assigns $\mathbf{x}$ to the class with the most representatives within the set of $k$ nearest vectors (Webb & Copsey, 2011). The choice of $k$ is a compromise between a value large enough to negate the effect of noise in the data yet small enough so that the neighbourhood does not extend into the domain of other classes. This value is typically optimised through some cross-validation process.

## 3.5 Feature Selection

Feature selection is performed to identify a minimally sized subset of given features. This can be done to reduce potentially computationally-demanding datasets into an optimally selected subset or to remove irrelevant or redundant features. The following criteria are generally adhered to when selecting this subset: the selected subset does not significantly decrease the classification accuracy and, given the class distribution or grouping, the values of the features selected best represent the original class distribution when all features are included (Dash & Liu, 1997).

A multitude of feature selection techniques have been proposed. The more common and those of interest for this study include sequential forward (SFS) and sequential backward (SBS) selection, sequential forward (SFFS) and sequential backward (SBFS) floating selection, and branch-and-bound feature selection (Jain & Zongker, 1997).

Forward and backward feature selection methods begin with a feature subset and iteratively add or remove features until some criterion has been met. A shortfall of these techniques is that all

possible subsets may not be examined due to the criterion, resulting in nested sub-optimal feature subsets that cannot be corrected later. Consequently, an optimal subset may not be achieved.

This "nesting" problem is addressed through a technique called the *plus l – take away r* method, which itself is a combination of the SFS and SBS methods discussed. The *plus l-take away r* method employs the SFS *l* times followed by SBS *r* times and repeats this step until some criterion function has been satisfied (Kittler, 1986). This allows for retrospective evaluation of the feature selection steps in an attempt to better optimise the final feature subset.

However this retrospection is limited by the fixed values of *l* and *r*, and it is argued that this "nesting" problem can only be partially overcome using this method (Pudil, Ferri, Novovicova, & Kittler, 1994). Sequential forward (SFFS) and sequential backward (SBFS) floating selection aims to control this conditional inclusion and exclusion based on the value of the criterion itself. The inclusion/exclusion criterion between the *plus l – take away r* and sequential floating selection methods is the fundamental difference (Figure 3.4).

It is carried out by first performing, say, sequential forward selection, after which sequential backward selection is carried out. SBS is carried out iteratively, evaluating the subset after each SBS step. SBS is halted at that point where that subset is no better than the subset produced by the preceding SBS step. The same can be performed with an initial sequential backward selection step followed by iterative sequential forward selection. This retrospective selection is dynamically controlled and hence no parameter need be set for this feature selection method.

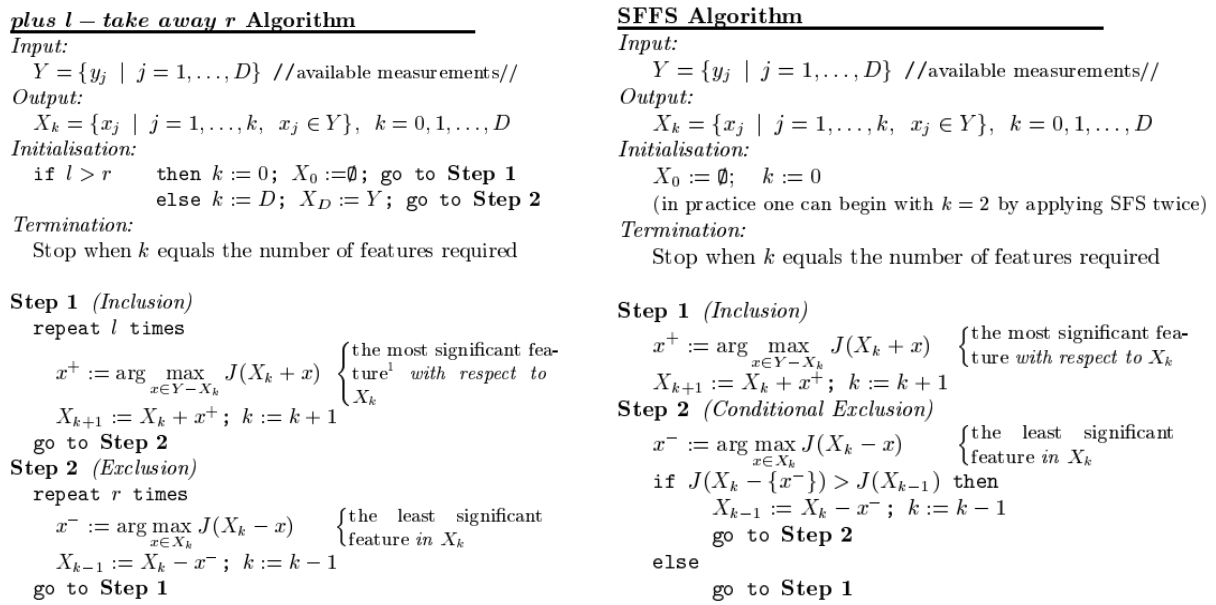


**Figure 3.4: The *plus l – take away r* and SFFS algorithms showing the fixed versus dynamic criterion** (adapted from Pudil et al., (1994))**.**

Branch and bound feature selection has been likened to a tree with the root being the full dataset of $n$ features and branches being subsets of this root (Narendra & Fukunaga, 1977). An optimal subset of $m$ features is obtained by evaluating defined subspaces of the original dataset using some given feature selection criterion function $J_{\bar{m}}(Z_1, \cdots, Z_{\bar{m}})$, where $(Z_1, \cdots, Z_{\bar{m}})$ are the $\bar{m}$ features to be discarded to achieve the subset $m$. For each feature included in the subset, the upper and lower bounds of the criterion function $J_{\bar{m}}$ are recalculated. If a feature satisfies the boundary conditions the algorithm proceeds to the next succeeding feature in the branch. The same evaluation using the criterion function and bounds is carried out on this succeeding feature and all succeeding features in the branch until the highest level in the branch is reached. This is carried out for different groups of features, the group distribution dictated by some given variables within the dataset. For those features where the conditions of the criterion function are not met, it is assumed that any feature combinations succeeding that feature will also not satisfy the criterion function and that branch is rejected and another branch of features is explored. The flow diagram in Figure 3.5 outlines the progression of branch and bound feature selection.

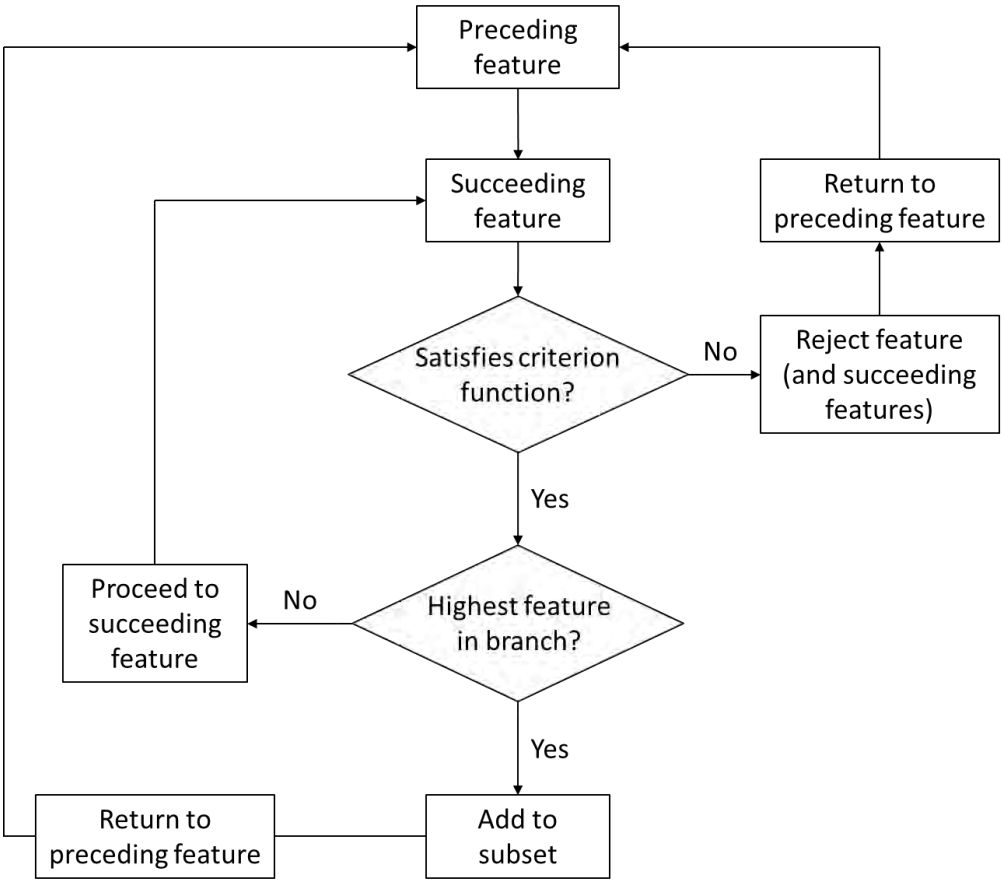


**Figure 3.5: Flow diagram illustrating the progression of branch-and-bound feature selection** (adapted from Narendra & Fukunaga (1977))**.**

# 4. Stereophotogrammetry Imaging System

The stereophotogrammetry system used in this study has several components – a camera system and calibration rig for image capture and interpolation of craniofacial landmarks (Figure 4.1), proprietary image processing software, landmark triangulation software and statistical shape analysis software.

**Figure 4.1: The stereophotogrammetry imaging system**

The system was designed and constructed at the University of Cape Town and a version of it has been used previously in studies seeking to characterise craniofacial dysmorphology in children with foetal alcohol syndrome (FAS) (Mutsvangwa et al., 2009, 2010).

## 4.1 Stereophotogrammetry Rig Design

The stereophotogrammetry system consists of two major physical components, the camera rig and calibration rig. The camera rig captures a set of three images simultaneously from central (frontal), oblique left and oblique right orientations. The images contain the subject's head and face and the surrounding calibration frame (Figure 4.2).

**Figure 4.2: Example of an image set including images from the left, centre and right cameras.**

### 4.1.1 Camera Rig

The camera frame and tripod are of bespoke design. A camera frame, made up of two metal plates connected via vertical struts, holds three digital single-lens reflective (DSLR) cameras. Three DSLR cameras (Canon EOS 1000D with 18-55mm variable lens) are mounted in the camera frame. Each camera is connected to a Canon ACK-E5 AC adapter kit, ensuring the cameras are continuously online. A vinyl clamp, tightened using an Allen key, is fitted to each camera lens to ensure the focal length and focus is fixed. A trigger hardwired to each camera fires all three cameras simultaneously and is also mounted on the camera frame. Each camera is removable from the frame for camera calibration purposes (Figure 4.3).

**Figure 4.3: The camera rig**

The image produced by each camera is 10.1 mega-pixels with a resolution of 3,888 x 2,592 pixels and is produced in RAW format. The cameras are set with a high shutter speed and low aperture (1/60 and F5.6, for example) and with the camera flashes engaged to maximise image quality.

### 4.1.2 Calibration Rig

The calibration rig consists of a calibration frame secured to a seat (Figure 4.4).

**Figure 4.4: The calibration rig**

The calibration frame consists of two components, the control frame and backbone frame. Both frames contain 5mm retro-reflective markers (3M Scotchlite, Minnesota) strategically placed with known coordinates in three-dimensional space. The markers on the control frame (control markers) surround an "area of best interpolation", a space where the craniofacial region of each study participant should be positioned to optimise craniofacial landmark interpolation. The markers on the backbone frame (check markers) fall inside this area of best interpolation (Figure 4.5).

Both sets of markers are used in conjunction for camera calibration by interpolating the positions of the check markers using the control markers and comparing the resulting check marker coordinates with their previously calibrated coordinates. Only the control markers are used for landmark

interpolation as the participant's head obstructs check markers (Figure 4.2). The entire frame is fixed to a seat where all subjects will be placed during image acquisition.

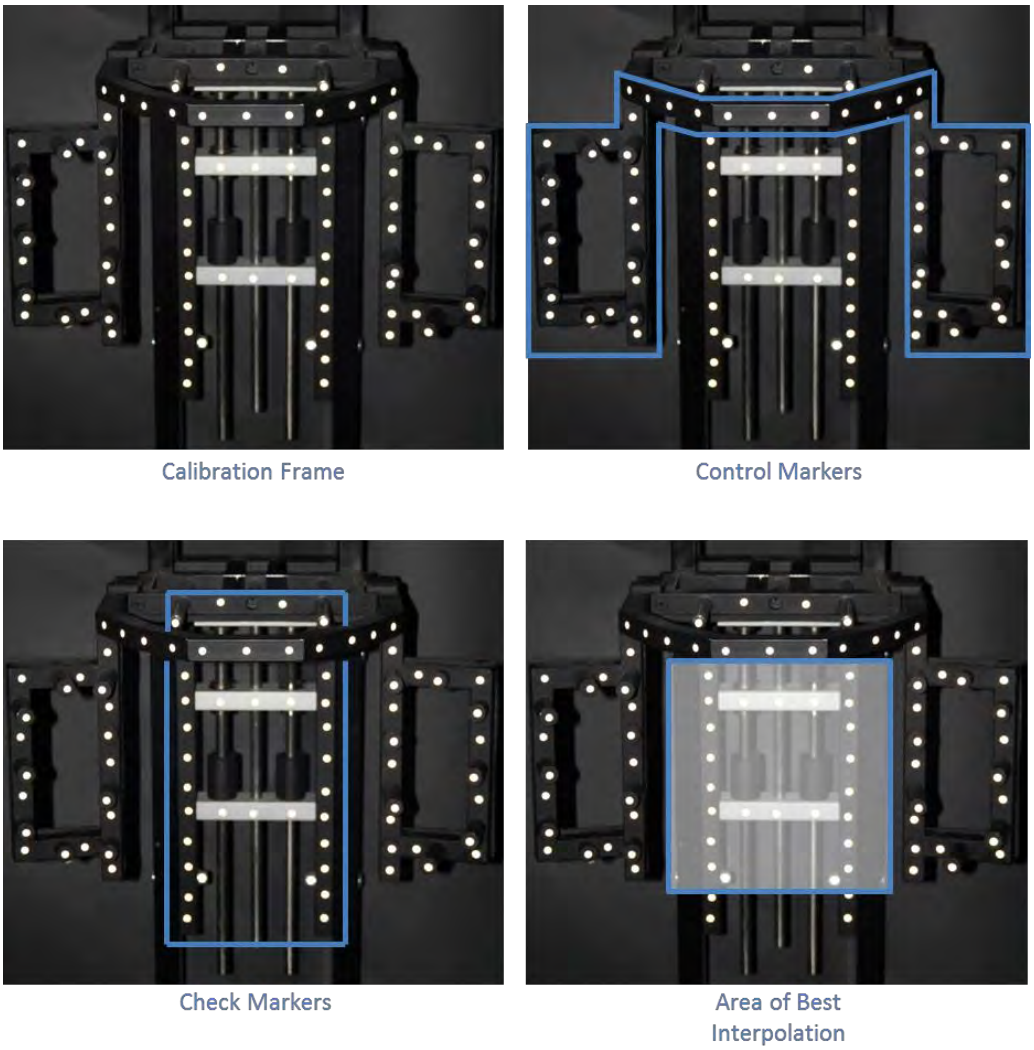


**Figure 4.5: The calibration frame with control and check markers and area of best interpolation.**

The height of the control marker frame is adjustable to account for the varying height of the subjects. However, adjusting the frame height changes the position of the markers relative to the cameras, and consequently recalibration of the cameras would be required for the adjusted relative marker positions. Rather, the seat where each subject sits is adjusted such that their head falls within the area of best interpolation. The frame is bolted to this seat.

## 4.2 Software Used in Analysis

The RAW images are imported into Canon Digital Photo Professional Version 3.8.0.0. The images are processed where necessary, adjusting the image properties to optimise the craniofacial features of each subject.

### 4.2.1 Australis

Australis is a software package for close-range digital photogrammetry. It is designed to carry out automated off-line measurement from convergent digital image networks and produce three-dimensional point object coordinates and calibration data (Photometrix, 2004). To carry out the 3D measurement operation, the software requires a number of convergent images of the subject and coded targets from which to carry out the measurement, in this instance the control frame markers. The coded targets are identified using an imported file of the target coordinates. Then the craniofacial landmarks are manually located using a point-and-click method. The control frame marker 3D coordinates are used to interpolate the coordinates of the selected craniofacial coordinates.

Triangulation and bundle adjustment functions aid in improving the accuracy of these coordinates. Triangulation is a method of 3D coordinate determination involving the simultaneous orientation of all points identified in all images (Luhmann, Robson, Kyle, & Harley, 2006). Bundle adjustment is a least-squares estimation procedure that computes the orientation of the cameras and in doing so determines the 3D coordinates of all the landmarks (Photometrix, 2007).

#### 4.2.1.1 Landmark Error Management Using Australis

As stated previously, landmark identification using Australis is a manual point-and-click method. Consequently, there is a degree of subjectivity in this method which may lead to landmark inaccuracies. The use of three images for triangulation aids qualitatively with landmark errors. Two images are all that is required to triangulate landmark coordinates. The third image is used to verify the correct positioning of the landmarks in the previous two images. This is achieved through the functionality of the Australis software, which, along with the landmark coordinates, produces the RMS error for each landmark. Iterative landmark placement is carried out to minimise this RMS error. If the operator observes the third image landmark moving away from the desired landmark in order to minimise this RMS error, this indicates an error in landmark placement in the first two images. This must be corrected and then this process repeated until the operator is satisfied that the landmark in the third image falls on the desired point in concert with a decreasing RMS error.

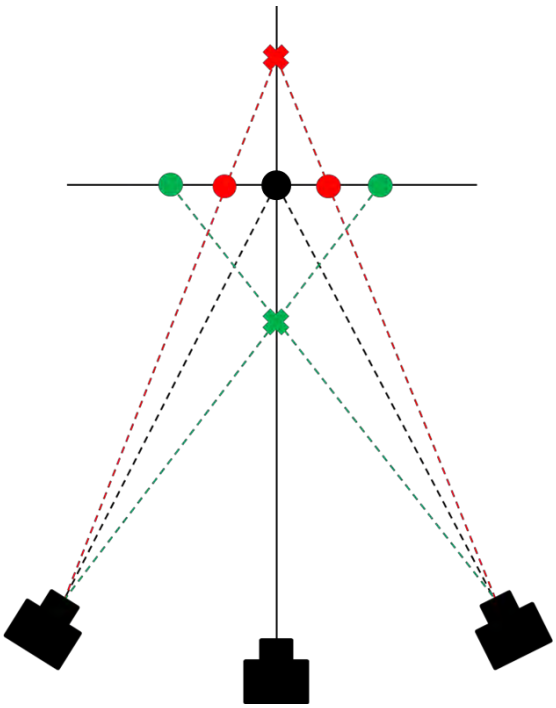

**Figure 4.6: Illustration highlighting the effect of landmark estimation error and the use of three cameras to minimise such an error.**

Figure 4.6 illustrates the use of the third camera to check landmark error. Consider a landmark placed in the first image captured by the central camera (*black X*). Landmarks can be placed manually or detected by software. This landmark is then located in a second image captured by either of the lateral cameras. If this landmark is erroneously positioned (*green or red dot*), the triangulation yields false landmark coordinates (*green or red X*). Positioning this landmark in the third image is in fact a practice of locating the first two landmarks, carried out, as previously stated, by finding that point that minimises the RMS error. If there is an error in the landmark positions in the first two images, the operator will observe a greatly misplaced landmark on the image plane (*green or red dot*) of the third image from the desired landmark position and relative to the landmark positions of the first two images.

### 4.2.2 MorphoJ

The MorphoJ software (Klingenberg, 2011) offers a platform for morphometric analysis of the 3D landmark data extracted using Australis. The features of this software package to be used in this project are the Procrustes analysis, principal component analysis and discriminant function analysis functions; these are described in Chapter 3.

### 4.2.3 PRTools in Matlab

PRTools is a pattern recognition toolbox used with Matlab (MATLAB 8.2, The MathWorks Inc., Natick, MA, 2013). It offers multiple feature selection as well as linear, density based and nonlinear classification functionalities (Duin et al., 2007). Additionally, PRTools has encoded predefined feature criteria as previously discussed, such as Mahalanobis and Euclidean distances. Mahalanobis distance is described as the distance between an object and the centroid of each group in the $n$-dimensional space defined by $n$ variables (Garson, 2012). Euclidean distance is merely the distance between two points in 3-dimensional space.

## 4.3 Calibration of the Marker Coordinates

As previously mentioned, the control markers serve as 3D reference coordinates for craniofacial landmark measurement purposes while both the control and check markers are utilised in camera calibration.

The frame was calibrated previously, placing it within a laboratory calibration grid at the UCT Geomatics Department and using the calibration process described in (Mutsvangwa et al., 2009). The 3D grid coordinates were known to within 0.1mm. A series of high definition highly convergent images of the frame and calibration grid were obtained and imported into the Australis software to determine the 3D coordinates of the frame. The reflective markers were identified using a simple point-and-click method and the Australis software automatically determined the centre of each marker. Bundle adjustment was then carried out to improve the accuracy of these marker coordinates.

The calibration frame enables interpolation of 3D coordinates within the frame boundary. The coordinates of the check markers lying within the area of best interpolation were interpolated using the control marker coordinates and compared to the known check marker coordinates determined using the laboratory calibration grid. The comparison validated the interpolation capabilities of the frame's control markers.

# 5. Precision and Reliability of the Stereophotogrammetry System

The measure of reliability and precision indicates the quality of the anthropometric system. Weinberg et al. (2004) stated that the "ability to obtain reliable and accurate measurement data is perhaps the most important criterion upon which to evaluate any measurement technology". It is for this reason that the stereophotogrammetry tool utilised in this project underwent rigorous testing to evaluate the precision and reliability, prior to its implementation in an anthropometric study.

Precision is the reproducibility of the same measurement between iterations. Reliability is the ability to produce a measurement truly representative of the parameter being measured (JCGM, 2012). A precise but unreliable measurement illustrates a quantity repeatedly produced which does not truly represent the parameter in question. A reliable yet imprecise measurement indicates a quantity produced true to the parameter measured, but shows an inconsistency in measurement of that quantity between iterations.

While no benchmark is required against which to test precision, which is the merely a comparison of repeated measurements of the same entity, reliability can only truly be measured if the value of the entity measured is known. Direct anthropometry is regarded as the gold standard for testing the reliability of other anthropometric measurement techniques, or at the very least the modality of measurement against which others are most commonly compared (Aung, Ngim, & Lee, 1995; Weinberg, Scott, Neiswanger, Brandon, & Marazita, 2004; Wong et al., 2008).

## 5.1 Methods of Precision and Reliability Measurement

Several methods for measuring precision are used in anthropometry. Two of these used previously with the stereophotogrammetry system implemented here are mean absolute difference (MAD) and relative error of magnitude (REM).

For a given measurement, mean absolute difference is calculated by averaging the absolute difference between the same measurement for all subjects between taken at different intervals (Mutsvangwa, 2009). The operation is simple to calculate, requires few assumptions regarding the data, easily interpreted for comparative purposes (the outcome is in its original unit of measure) and is independent of the size of the measurement. Relative error of magnitude is the ratio between MAD and the grandmean, the overall average of all measurements in a sample across all iterations. REM represents the estimate of error magnitude relative to the size of the measurement and expressed as a percentage (Weinberg et al., 2004).

$$REM = \frac{MAD}{grandmean} \times 100$$

Intra- and inter-operator precision must be assessed. Intra-operator precision is a measure of the regularity of the same measurement made by the same operator at different time intervals, while inter-operator precision indicates the regularity of the same measurement made by different operators. In both cases, the same modality of measurement is used.

The reliability of the system is assessed comparing those measurements of the measurement modality in question with the gold standard, which in this case is direct anthropometry. This is assessed using the criteria defined by Aung et al. (1995). Inter-modality measurement disparities are categorised as highly reliable (<1.0mm), reliable (1.0 – 1.5mm), moderately reliable (1.6 – 2.0mm) and unreliable (>2.0mm) (Aung et al., 1995).

## 5.2 Previous Precision and Reliability Testing of the Stereophotogrammetry System

The calibration frame used in this project was designed as part of a stereo-photogrammetric system by Mutsvangwa et al. (2009) to study the facial phenotype associated with foetal alcohol syndrome. In the study, REM methods as described above employing direct anthropometry and the stereophotogrammetry system were used to assess precision and reliability. Proportional error of measurement, a function similar to REM, but with a grandmean calculated from both measurement modalities, was performed to normalise each operator's inter-modality reliability. Two operators carried out the tests using both modalities at two separate intervals.

A scoring system for precision was used to assess the test results as follows. Scores less than 1% from the mean were deemed "excellent", between 1 and 3.9% as "very good", between 4 and 6.9% as "good", between 7 and 9.9% as "moderate" and greater than 10% as "poor". The normalised inter-modality reliability tests yielded measurements of which 88.8% were at least "very good". Direct anthropometry and stereophotogrammetry inter-operator precision showed measurements deemed at least "very good" of 93.1% and 99.6% respectively.

Mutsvangwa et al. (2009) showed that the stereophotogrammetry system developed is highly precise and reliable and that data collected using the system can be analysed and reported with a high level of confidence.

## 5.3 Precision and Reliability Test Implementation

The precision and reliability tests described above were repeated for this study for two reasons. While some landmarks used in this study were the same as used previously, they were not identical. Also, several years had passed since the system was used in the previous study. The change in methodology and time period between previous and current studies warranted re-examination of the system's precision and reliability.

A single subject was used with nine landmarks highlighted with a felt-tip marker along the midline of the face prior to testing. The landmarks chosen for this test are a subset of the landmarks used later for the assessment of craniofacial dysmorphology. This set was chosen to achieve some continuity between these tests and later geometric morphometric analysis of the study cohort. No measurements were taken about the eyes to minimise the risk of harm as a result of the use of callipers around this area. Measurements were taken using callipers as well as the stereophotogrammetric system by two operators at two different intervals.

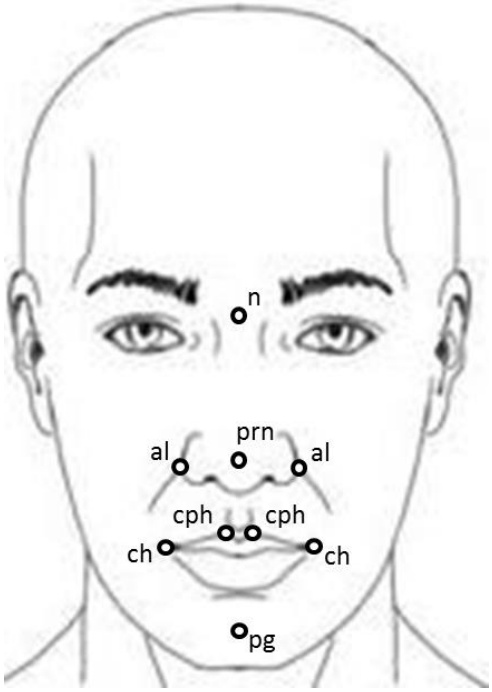


**Figure 5.1: Craniofacial landmarks for precision and reliability testing. al, alare; ch, cheilion; cph, christa philtrum; n, soft tissue nasion; pg, pogonion; prn, pronasale**

The following measurements were carried out directly by each operator on separate occasions using callipers.

1. Soft tissue nasion to alare (n – al)
2. Pronasale to alare (prn – al)
3. Alare to christa philtrum (al – cph)
4. Christa philtrum to cheilion (cph – ch)
5. Cheilion to pogonion (ch – pg)
6. Soft tissue nasion to pogonion (n – pg)
7. Between the christa philtrum (cph – cph)

Images of the subject were taken using the stereophotogrammetry system. The images were digitally landmarked using the Australis software and those landmark coordinates then used to determine the same inter-landmark distances as determined using the direct method.

REM scores were calculated to determine intra- and inter-operator precision while the scale developed by Aung et al. (1995) and the proportional error of magnitude were used to determine inter-modality reliability, similar to Mutsvangwa et al. (2009).

## 5.4 Precision and Reliability Results

Detailed results of intra- and inter-operator precision and normalised inter-modality reliability are given in Appendix A. Only the precision of the stereophotogrammetry system was analysed. We have not assessed the precision of direct anthropometry as it is the efficacy of the stereophotogrammetric system that is the focus of this study.

### 5.4.1 Precision of the Stereophotogrammetry System

Table 5.1 below presents the performance of the precision tests.

| Rating | Intra-Operator Precision | Inter-Operator Precision |
|---|---|---|
| Excellent | 43% | 71% |
| Very good | 57% | 14% |
| Good | 0% | 14% |
| Moderate | 0% | 0% |
| Poor | 0% | 0% |

**Table 5.1: Precision tests – performance of the stereophotogrammetry system**

Both the intra-operator precision, the ability of each operator to reproduce the same measurements at different intervals, and inter-operator precision, the ability of the two operators to produce measurements similar to each other, were high. 100% and 85% of measurements were rated at

least “very good” for intra- and inter-operator precision respectively, while no measurements were rated below “good”.

For inter-operator precision, Mutsvangwa (2009) reported results of “very good” or better to account for 99.6% of all measurements (versus 86% in this study).

Mutsvangwa (2009) did not compare intra-operator precision as above, but did report on intra- and inter-operator differences, reporting differences along all axes to be less than 0.9mm and 0.6mm respectively. The intra- and inter-operator differences along all axes for both operators are shown in Figure 5.2 and Figure 5.3. All intra-operator differences were less than 1.9mm. All inter-operator differences were less than 2.1mm.

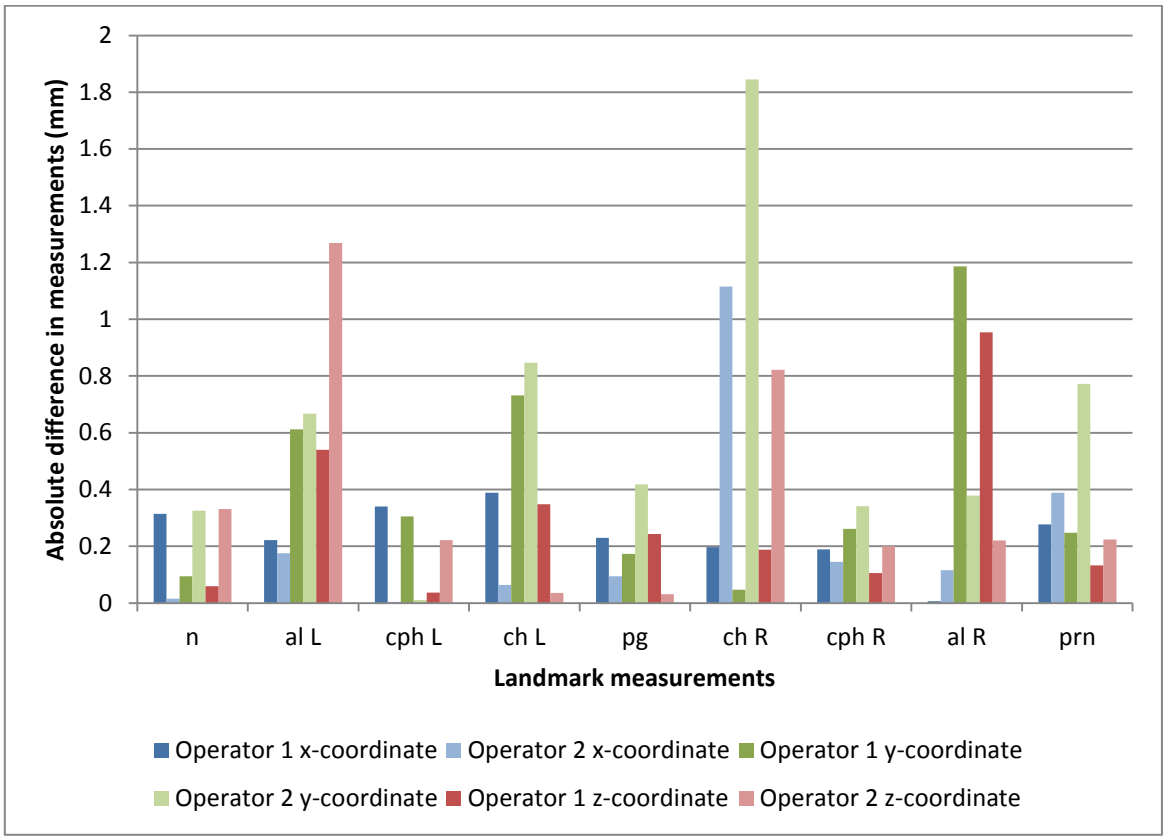


**Figure 5.2: Intra-operator differences**

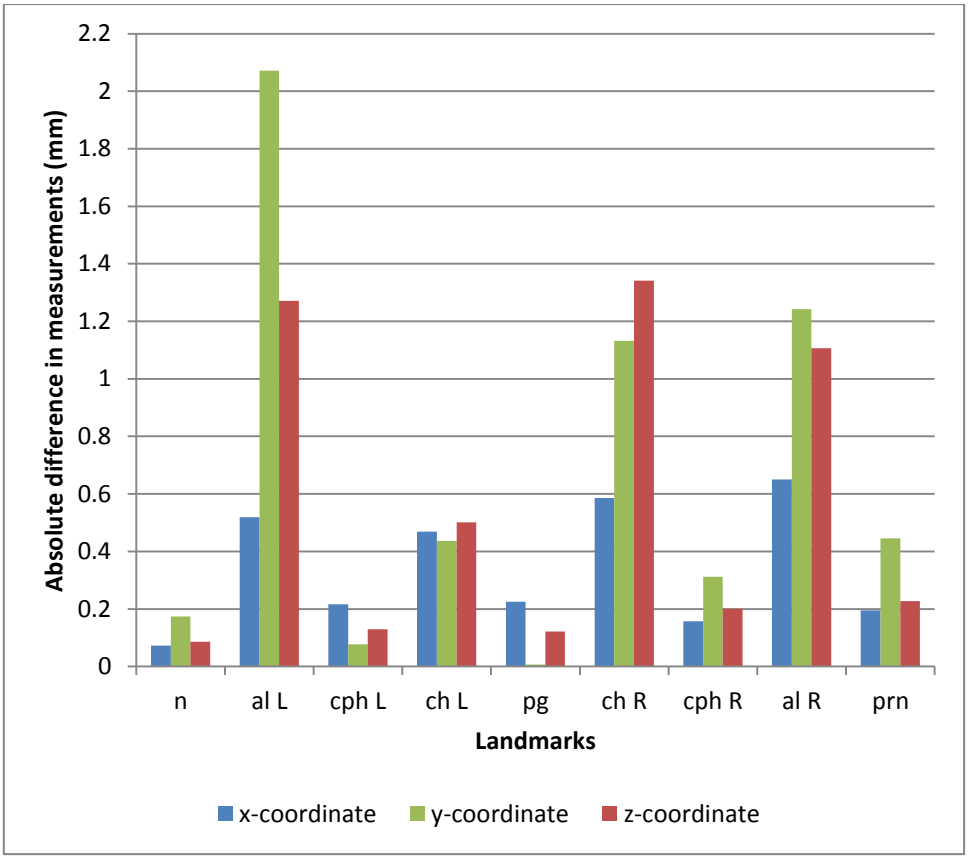


**Figure 5.3: Inter-operator differences**

The previous study outperformed the current study, however the current precision ratings are still very encouraging. The worst performing landmarks were both alare and the right cheilion. Each alare, the most lateral point of the nose, is only visible in two of the three images. This negatively affects landmark placement which could explain the poor precision. The cheilion is a very identifiable landmark, being the commissure of the mouth. The fact that only the right cheilion performed poorly may be attributable to uneven lighting leading to poor identification.

It should be noted that the previous study carried out the precision and reliability analysis using a single inanimate hard plastic doll. The use of an inanimate object means that the observer need not be concerned for the wellbeing of the subject nor do they need to be concerned with potential deformation of soft tissue when performing direct measurements using callipers. Additionally, an inanimate object will not move during image acquisition while there is no guarantee that a live subject will remain still. These key differences between the two studies may have contributed to the better precision and reliability outcomes in the former.

### 5.4.2 Reliability of the Stereophotogrammetry System

Figure 5.4 below shows the absolute differences in measurements taken using direct methods and the stereophotogrammetry system.

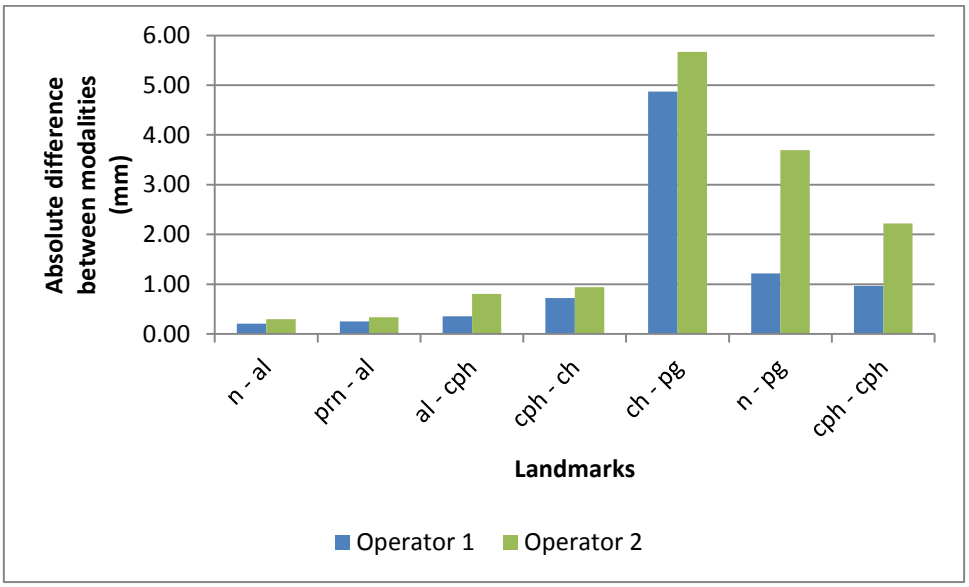


**Figure 5.4: Inter-modality differences**

Absolute differences for soft tissue nasion-to-alare (*n-al*), pronasale-to-alare (*pr-n*), alare-to-crista philtrum (*al-cph*), and christa philtrum-to- cheilion (*cph*-ch) measurements were less than 1mm, scored as "very reliable" for both operators. For at least one of the operators, the remaining cheilion-to-pogonion (*ch-pg*), soft tissue nasion-to-pogonion (*n-pg*) and christa philtrum-to-christa philtrum (*cph-cph*) exceeded 2mm, scored as "unreliable".

Table 5.2 below presents the performance of the reliability tests.

| Rating | Normalised Inter-Modality Reliability |
|---|---|
| Excellent | 21% |
| Very good | 50% |
| Good | 7% |
| Moderate | 0% |
| Poor | 21% |

**Table 5.2: Reliability test – performance of the stereophotogrammetry system**

Mutsvangwa (2009) reported normalised inter-modality reliability ratings of "very good" or better to account for 89% of all measurements while the current study can report only 71% for the same. 21% of measurements were deemed "poor", with the cheilion-to-pogonion (*ch-pg*) and christa philtrum-to-christa philtrum (*cph-cph*) measurements proving the poorest for both operators. Note that once normalised, the largest measurement of nasion-to-pogonion (*n-pg*) now scores "very good".

The pogonion is described as the point located most anteriorly on the chin (Farkas, 1994). Landmarks such as this are referred to as soft landmarks due to the lack of identifiable reference points to aid identification, for example, the commissures of the eyes or mouth. This leads to operator subjectivity when identifying the landmark and could explain the poor outcome of the *ch-pg* measurement.

The christa philtrum is described as the point on the lateral margin of the philtrum on the upper vermilion border (Farkas, 1994) and hence should be easier to identify than, say, the pogonion. However the *cph-cph* measurement was the smallest measurement observed, in fact, almost half the magnitude of the next smallest measurement. Smaller measurements are less robust and any error that does occur is reflected moreso than larger measurements. This could explain the poor outcome of the *cph-cph* measurement.

If these two measurements were to be excluded, the remaining measurements yield excellent results with 100% of ratings would be “very good” or better, illustrating, with the exception of the landmarks as described above, that the system can be highly reliable.

The stereophotogrammetry system proved satisfactory in terms of precision and reliability. However, going forward special care must be taken when identifying soft landmarks such as the pogonion.

# 6. Study Methodology

This chapter discusses the overall methodology followed in the study. Participant selection and image digitisation are presented and also discussed are landmark extraction and geometric morphometric analysis, as well as the software used to carry out each.

## 6.1 Participant Selection and Image Acquisition

Participants for this study were selected from those available for a larger study, which recruited patients diagnosed with schizophrenia, schizoaffective disorder and bipolar disorder from Valkenberg Hospital over a three-year period. All selected patients were interviewed and satisfied the criteria set out in the 4$^{th}$ Diagnostic and Statistical Manual (DSM-IV) and 10$^{th}$ International Classification of Diseases (ICD-10) for the disorders described above. Control patients were members of the staff of Valkenberg Hospital, a public psychiatric hospital, and the student population of the University of Cape Town. All participants were interviewed in accordance with the Structured Clinical Interview for DSM-IV Axis I Disorders (SCID-I) to confirm initial diagnosis in patients and screen controls for psychosis. The interviews were performed by trained psychiatrists at Valkenberg Hospital. Written consent was given by all participants when in a lucid state.

Participants were photographed using the stereophotogrammetric tool. They were seated in the calibration rig with their head within the area of best interpolation (as described in Section 4.1.2). It was ensured that each participant presented with the correct pose for image acquisition: head upright, an expressionless pose, mouth closed with teeth lightly occluding, hair tied back and with no make-up, glasses or jewellery. Several image sets were captured of each subject to help ensure that a suitable image set was obtained. Incorrect pose can affect landmark extraction by distorting those landmarks selected and ultimately compromising the reliability of the data (Mutsvangwa, 2009).

All interviews and image acquisition took place at Valkenberg Hospital.

Only participants diagnosed with schizophrenia were included in this study, and 47 image sets were divided into African and Caucasian control and schizophrenia groups. Of these, one was excluded due to poor image quality (even after multiple images of the subject were captured), one was excluded due to incorrect pose and one was excluded due to difficulty with image post-processing, leaving 44 viable image sets for analysis. The male African group accounted for 17 of these image sets, the male Caucasian group for 13, the female African group for 9 and the female Caucasian group for 5 (Table 6.1).

| African | | | | Caucasian | | | |
|---|---|---|---|---|---|---|---|
| Male | | Female | | Male | | Female | |
| 17 | | 9 | | 13 | | 5 | |
| Control | Schiz. | Control | Schiz. | Control | Schiz. | Control | Schiz. |
| 8 | 9 | 5 | 4 | 8 | 5 | 5 | 0 |

**Table 6.1: Study cohort**

Both the female groups were excluded from analysis. The African female group consisted only 9 participants raising concerns about the group's lack of statistical power. The Caucasian female group contained no schizophrenia participants so no comparative analysis could be carried out at all.

## 6.2 Landmark Extraction

The images acquired were assessed for image quality and correct subject pose, with those not satisfying both criteria discarded. Image correction was carried out where necessary using Canon Digital Photo Professional Version 3.8.0.0, where sharpness, contrast and brightness could be adjusted to best aid in landmark identification and extraction.

The selected and corrected image set was loaded into the Australis software where a set of landmarks was identified using a mouse point-and-click approach. The landmarks are shown in Figure 6.1.

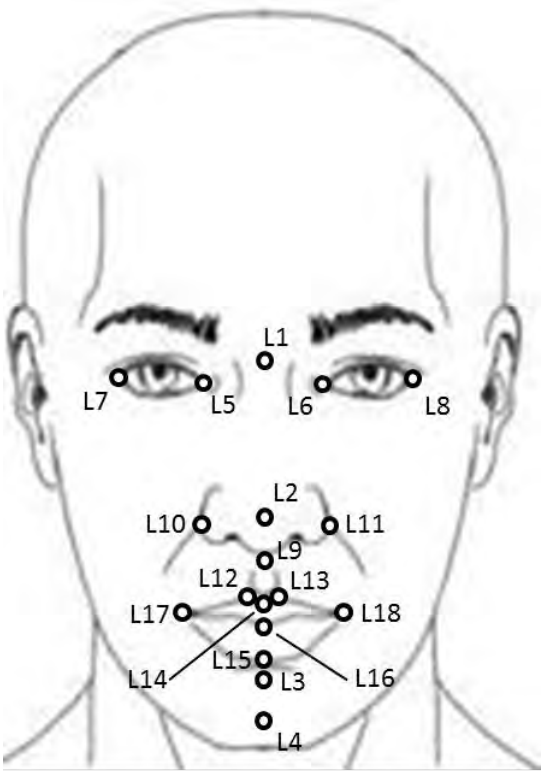


L1 – nasion
L2 – pronasale
L3 – sublabiale
L4 – pogonion
L5 & L6 – endocanthion
L7 & L8 – exocanthion
L9 – subnasale
L10 & L11 – alare
L12 & L13 – christa philtrum
L14 – labiale superius
L15 – labiale inferius
L16 – stomion
L17 & L18 – cheilion

**Figure 6.1: The set of 18 landmarks.**

The selected landmarks were based on previous studies (Hennessy et al., 2007, 2010) and in line with established anthropometric guidelines (Farkas, 1994). Six landmarks included in the previous studies by Hennessy et al. were excluded from this study due to the inability to identify them in the images acquired. These six landmarks (left and right) are the columella breakpoint – the anteriormost point of the nostril; the tragion – the point in the notch just above the tragus of the ear; and the otobasion inferius – the most inferoanterior attachment of the earlobe to the face (Farkas, 1994).

The exclusion of the nasal landmark is non-critical as there remain four landmarks in this region for use in craniofacial morphometric analysis. The otobasion inferius was used previously for the calculation of pseudo-landmarks, an operation not carried out in, and as such non-critical, to this study. Phenotypic models that found faces to be generally broader in schizophrenia (Hennessy et al., 2007) were undoubtedly measured between left and right tragion. Unfortunately, it was not possible to replicate this measurement given the current stereophotogrammetry rig design.

Once the 18 landmarks were selected across all three images in the set, triangulation and bundle adjustment functions were run in the Australis software to produce a reliable 3D coordinate landmark configuration (Figure 6.2).

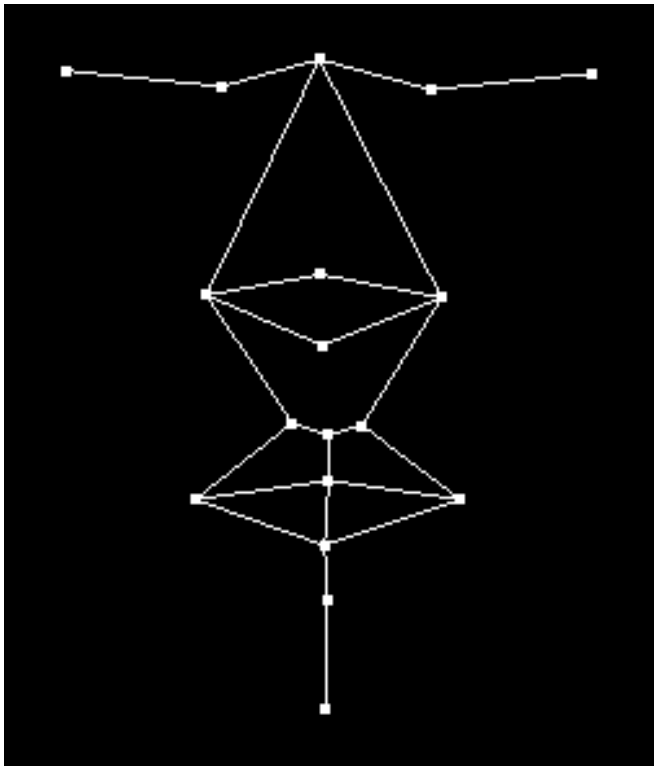

**Figure 6.2: Frontal view of the 18-point 3D coordinate landmark configuration generated in Australis.**

The bundle adjustment file, containing the 3D coordinates of the 18 landmarks, was then extracted for use in geometric morphometric analysis.

## 6.3 Geometric Morphometric Analysis of the Craniofacial Landmark Sets

The bundle adjustment files extracted from the Australis software were compiled into a single comma-separated value (.csv) file for the male African and male Caucasian groups in preparation for importing into the MorphoJ software. In addition, classifier .csv files were created to differentiate each of these groups into control and schizophrenia categories.

Geometric morphometric analysis for both groups was carried using the MorphoJ software, namely generalised Procrustes analysis, principle component analysis and discriminant function analysis.

Further analysis using feature selection and classification using the principle component scores ascertained using the MorphoJ software was executed using Pattern Recognition Tools (PRTools), a Matlab-based toolbox.

### 6.3.1 Procrustes Analysis

Procrustes analysis or Procrustes fit was performed to align all landmark configurations in the group, by applying the translational, rotational and scaling functions as described in Section 3.1. This produced the Procrustes residuals which would be used in principal component analysis.

After the Procrustes fit, symmetrical and asymmetrical covariance matrices are generated. The symmetrical matrix is produced with those landmarks that occur on either side of the craniofacial midline reflected about the midline and averaged. The asymmetrical matrix is produced with the original landmarks in order to retain the original shape matrices. Applying symmetry in this fashion is common is shape studies to remove the left-right shape differences (Klingenberg, 2011). The symmetric component is used to assess shape variation between specimens. The asymmetric component is used to investigate variation within a specimen, often about some midline. As such, the symmetric matrix is more pertinent to this study.

### 6.3.2 Principal Component Analysis

The covariance matrices are used in the execution of principal component analysis. Principal component scores were generated, calculated as vectors of deviations from the mean multiplied by their coefficients (eigenvectors).

A Jolliffe cut-off is often utilised in morphometric analyses (Jolliffe, 2002). This is a method of omitting those principal components that are shown to be insignificant. One such approach is to omit those principal components whose associated coefficients (eigenvalues) fall below some limit,

be it the mean of the eigenvalues or some percentage of the largest eigenvalue. This is left to the discretion of the investigator. Graphical applications of the Jolliffe cut-off may aid in the determination of which principal components to retain. The two most noteworthy graphs are scree and log-eigenvalue (LEV) graphs. A scree graph plots the eigenvalues of the respective principal components in decreasing order while the LEV graph does the same for the natural log of the principal components. Using the scree graph, the cut-off is determined by observing the first point of inflection or major gradient change or "elbow" and keeping those principal components preceding that elbow in the graph. The LEV graph, an exponential graph, tends towards a horizontal asymptote as the eigenvalues of the respective principal are plotted. That point where the graph reaches this horizontal is deemed the point after which the succeeding principal components are discarded.

The retained principal component scores may then be used when carrying out feature analysis.

### 6.3.3 Feature Analysis

The principal component scores were evaluated in an attempt to identify those features with greatest discriminatory power and then attempt to use those features to classify the objects into their discrete groups. Initially, discriminant function analysis (DFA), a classification method, was carried out without a preceding feature selection step. The analysis was then expanded to include other classification methods as well as feature selection techniques to reduce dimensionality of the PC score dataset and aid classification.

#### 6.3.3.1 Discriminant Function Analysis

Discriminant function analysis (DFA) seeks to classify two *a priori* groups of observations (Klingenberg, 2011).

DFA in MorphoJ is executed using Fisher's classifying rule as described in Section 3.4, a linear classification. DFA was carried out using all principal components from both cohorts and for both symmetrical and asymmetrical operations. The DFA provides information on the groups and the shape difference between them. Specifically, the analysis produces the Procrustes distance, the Mahalanobis distance, the T-square statistic and the parametric p-value. The Procrustes distance is the distance between the Procrustes shape coordinates of the two groups under scrutiny after Procrustes superimposition. The Mahalanobis distance is defined as a measure of the distance between two points in the space defined by two more or correlated variables. This distance is measured from the centroid of the mean shape of each group. The smaller the Mahalanobis number, the closer the subject to the centroid of the chosen group and the more likely

characterisation of that subject into that group (Garson, 2012). The T-square statistic is produced, comparing the centroid of each group against the null hypothesis that no difference exists between the centroids. The p-value is given to test against the null hypothesis that no statistically significant variation exists between the two groups.

If it is shown that statistically significant variation does exist, a dataset of the discriminant scores is produced, indicating which principal components have the discriminating power to classify individuals into groups.

#### 6.3.3.2 Feature Selection and Classification

Feature selection and classification were carried out using the MATLAB toolbox, PRTools (Duin et al., 2007). The MATLAB scripts for the execution of feature selection and classification described in this section are presented in Appendix C.

There are several feature selections available, most of which were discussed in Section 3.5. Due to the "nesting" issue as previously discussed, sequential forward and sequential backward selection were not implemented. Instead, sequential floating selection and branch-and-bound selection were implemented to identify those features yielding the greatest discriminatory power. The data input for this operation is the principal component scores calculated through the use of MorphoJ. Class labels were also imported, namely "Control" and "Schizophrenia". This was carried out for both the African and Caucasian cohorts.

As previously discussed, all feature selection techniques are subject to some feature criterion. A feature selection evaluation algorithm included in the PRTools software allows the user to evaluate the feature set of a dataset. Scores are awarded to each of the feature criteria. The highest scoring feature criterion is then used in feature selection to optimise the process. These different criteria are inter-intra distance, sum of estimated Mahalanobis distances, minimum of estimated Mahalonobis distance, sum of squared Euclidean distances, minimum of squared Euclidean distances and 1-nearest neighbour leave-one-out classification performance.

Visualisation of those principal components identified with the greatest discriminating power allowed qualitative description of craniofacial dysmorphology in schizophrenia compared to healthy controls.

The outputs from the feature selection are those principal component scores that are deemed the most discriminating between groups, removing redundant features.

These PC scores are used in classification to test whether objects within the dataset can be successfully classed based on their features. A range of classifiers (linear, polynomial, density based and nonlinear) were used in this study, in order to investigate the ability of each to assign an object to a class. Additionally, the successful execution of specific classifiers in previous craniofacial dysmorphology studies influenced the selection of classifiers. A previous study using a similar stereophotogrammetry system found success using nearest mean, Fisher, logistic linear (all linear) and quadratic Bayes (density based) classifiers (Mutsvangwa, 2009). A support vector machine classifier with radial basis function kernel was also successfully implemented in a study investigating craniofacial dysmorphology in Downs' syndrome (Zhao et al., 2013).

This study used the following classifiers: nearest mean classifier, logistic linear classifier, support vector classifier with radial basis function (RBF) kernel, quadratic Bayes classifier and k-nearest neighbour classifier. These classifiers are described in Section 3.4. Fisher's linear classifier was not chosen specifically as the DFA carried out is based on Fisher's algorithm.

To determine the success of classification, classification accuracy was analysed for each classifier to determine the likelihood of each classifier correctly assigning an object to its respective class. Due to the small sample size, leave-one-out cross-validation as described in Section 3.4 was utilised.

# 7. Results from Geometric Morphometric Analysis

A Procrustes fit (Figure 7.1) was performed for both groups and covariance matrices generated.

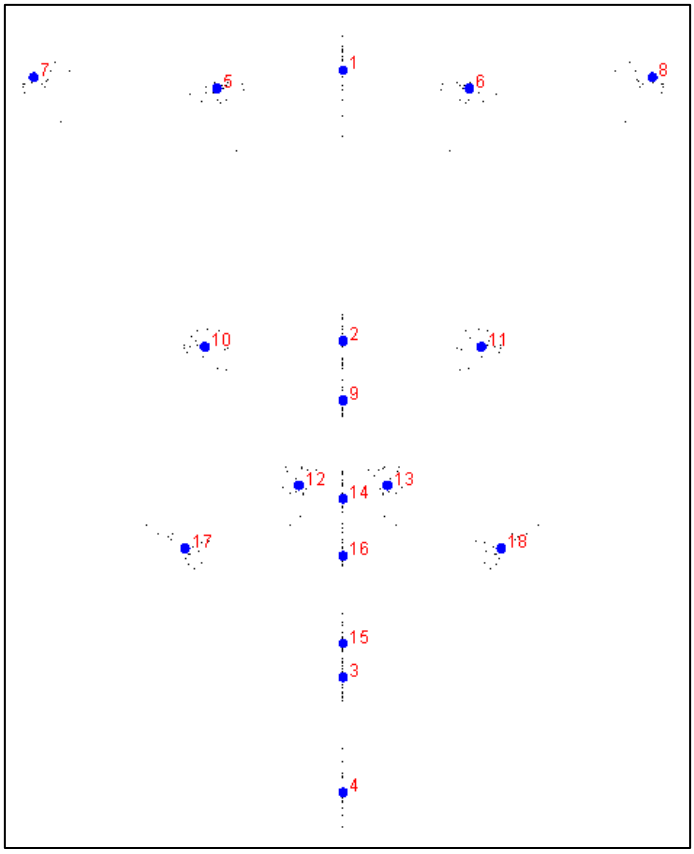


**Figure 7.1: Example of the Procrustes fit (frontal view). The large blue dot is the mean of each landmark. The small black dots are the landmarks for each subject. The numbers correspond to those assigned to the landmarks in Figure 6.1.**

## 7.1 Principal Component Scores

The covariance matrices were then used to perform PCA, which yielded the principal components (PCs) and their associated weighting (eigenvalues). 15 PCs were established for the African group and 11 for the Caucasian. The coordinates of all the PCs are tabulated in Appendix B. Table 7.1 and Table 7.2 below present the eigenvalues for each principal component, calculated using the symmetric covariance matrix. Additionally, the tables show each principal component's contribution to variance within the cohort, control and schizophrenia pooled together.

| PC | Eigenvalues | % Variance | Cumulative % |
|---|---|---|---|
| 1 | 0.002022 | 26.242 | 26.242 |
| 2 | 0.001229 | 15.959 | 42.201 |
| 3 | 0.001137 | 14.762 | 56.963 |
| 4 | 0.000808 | 10.493 | 67.457 |
| 5 | 0.000587 | 7.614 | 75.071 |
| 6 | 0.000499 | 6.475 | 81.546 |
| 7 | 0.000339 | 4.396 | 85.941 |
| 8 | 0.00026 | 3.376 | 89.317 |
| 9 | 0.000229 | 2.973 | 92.29 |
| 10 | 0.000178 | 2.313 | 94.604 |
| 11 | 0.000139 | 1.807 | 96.411 |
| 12 | 0.000117 | 1.516 | 97.926 |
| 13 | 0.000101 | 1.307 | 99.234 |
| 14 | 3.85E-05 | 0.5 | 99.734 |
| 15 | 2.05E-05 | 0.266 | 100 |

**Table 7.1: Male African cohort – The weighting (eigenvalue) of each PC and the contribution to shape variance**

| | Eigenvalues | % Variance | Cumulative % |
|---|---|---|---|
| 1 | 0.002406 | 29.994 | 29.994 |
| 2 | 0.001429 | 17.818 | 47.811 |
| 3 | 0.001269 | 15.814 | 63.625 |
| 4 | 0.000753 | 9.387 | 73.012 |
| 5 | 0.000655 | 8.167 | 81.179 |
| 6 | 0.00053 | 6.607 | 87.785 |
| 7 | 0.000483 | 6.014 | 93.8 |
| 8 | 0.00025 | 3.121 | 96.921 |
| 9 | 0.000116 | 1.449 | 98.37 |
| 10 | 7.05E-05 | 0.878 | 99.248 |
| 11 | 6.03E-05 | 0.752 | 100 |

**Table 7.2: Male Caucasian cohort – The weighting (eigenvalue) of each PC and the contribution to shape variance**

The tables show that, for the African cohort, the first nine of fifteen PCs contribute greater than 90% of the variance within the pooled African cohort. For the Caucasian cohort, the first seven of eleven PCs contribute greater than 90% of the variance within the pooled Caucasian cohort.

Attempts to determine a cut-off for each group were carried out by establishing scree and LEV graphs. The graphs are displayed in Figure 7.2 below.

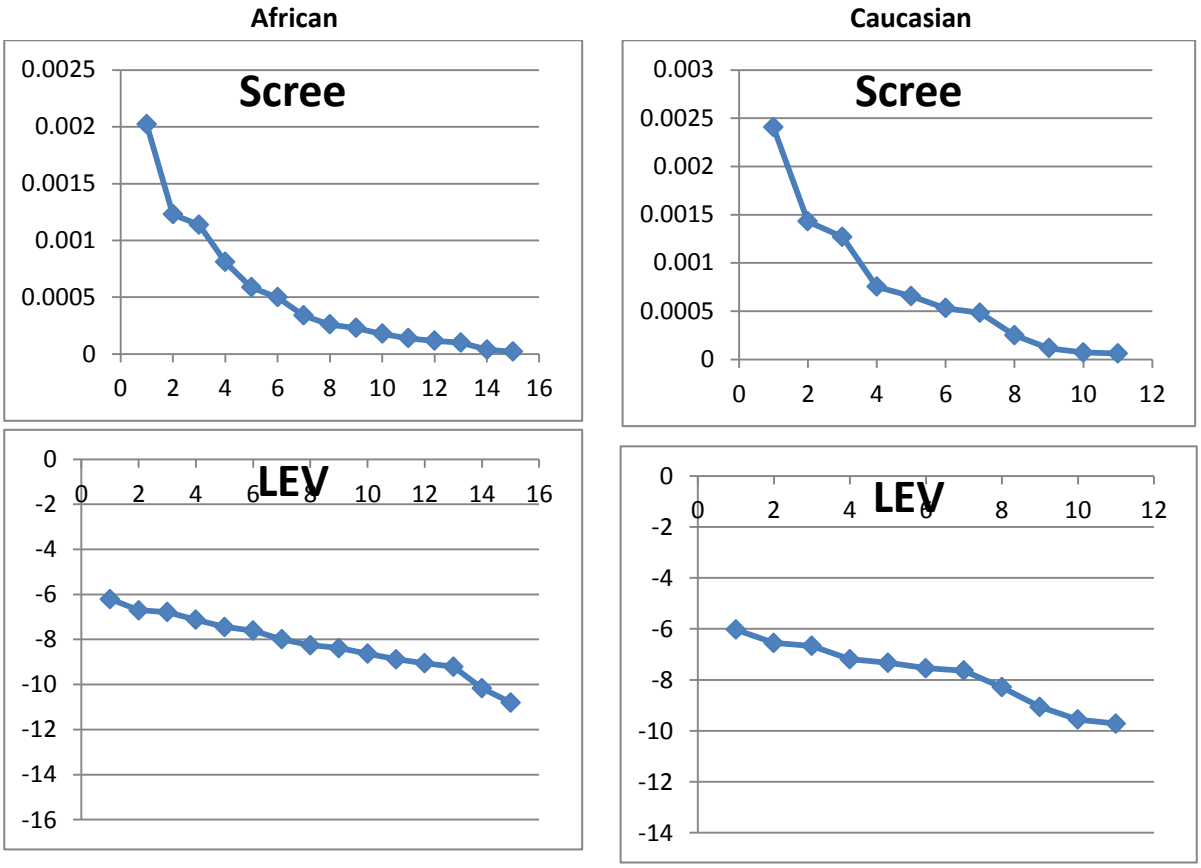


**Figure 7.2: Scree and LEV graphs for cut-off determination for the male group.**

The LEV graphs offer no assistance in selecting which PCs to retain and which to discard, remembering that the horizontal asymptote is chosen as the cut-off.

While the scree graphs do suggest cut-off points, these occur quite early in the graphs. For the African cohort, the graphs suggest retaining the first three and four of the fifteen PCs in the symmetric and asymmetric groups respectively. For the Caucasian cohort, the graph pertaining to the symmetric group suggests retaining only the first three of eleven PCs, while the graph pertaining to the asymmetric group does not show a clear point of inflection and hence one cannot determine which PCs to retain.

Ultimately, given the findings from the graphs and the relatively small number of PCs produced it was decided to retain all PCs for discriminant function analysis. In addition, the subtlety of the dysmorphology alluded to in the literature may require the inclusion of all PCs, regardless of their contribution to variance. The most subtle of variation may be the discriminating trait between the control and schizophrenia cohorts, however it must be noted that variation in lower order PCs may be a result of noise in the data rather than actual morphological variation.

## 7.2 Findings from Feature Analysis

The following findings were yielded from discriminant function analysis, branch-and-bound feature selection using Mahalanobis distance as the selection criterion and the various classifiers – nearest mean classifier, logistic linear classifier, quadratic Bayes normal classifier and k-nearest neighbour classifier.

### 7.2.1 Discriminant Function Analysis

The diagrams in Figure 7.3 are the result of discriminant function analysis of the principal components for the male African and Caucasian, symmetric covariance matrix. The illustrations overlay the mean shapes of the control and schizophrenia groups. The control group is shown with light blue lines and light blue landmarks. The schizophrenia group is shown with dark blue lines and solid dark blue landmarks. The differences have not been scaled.

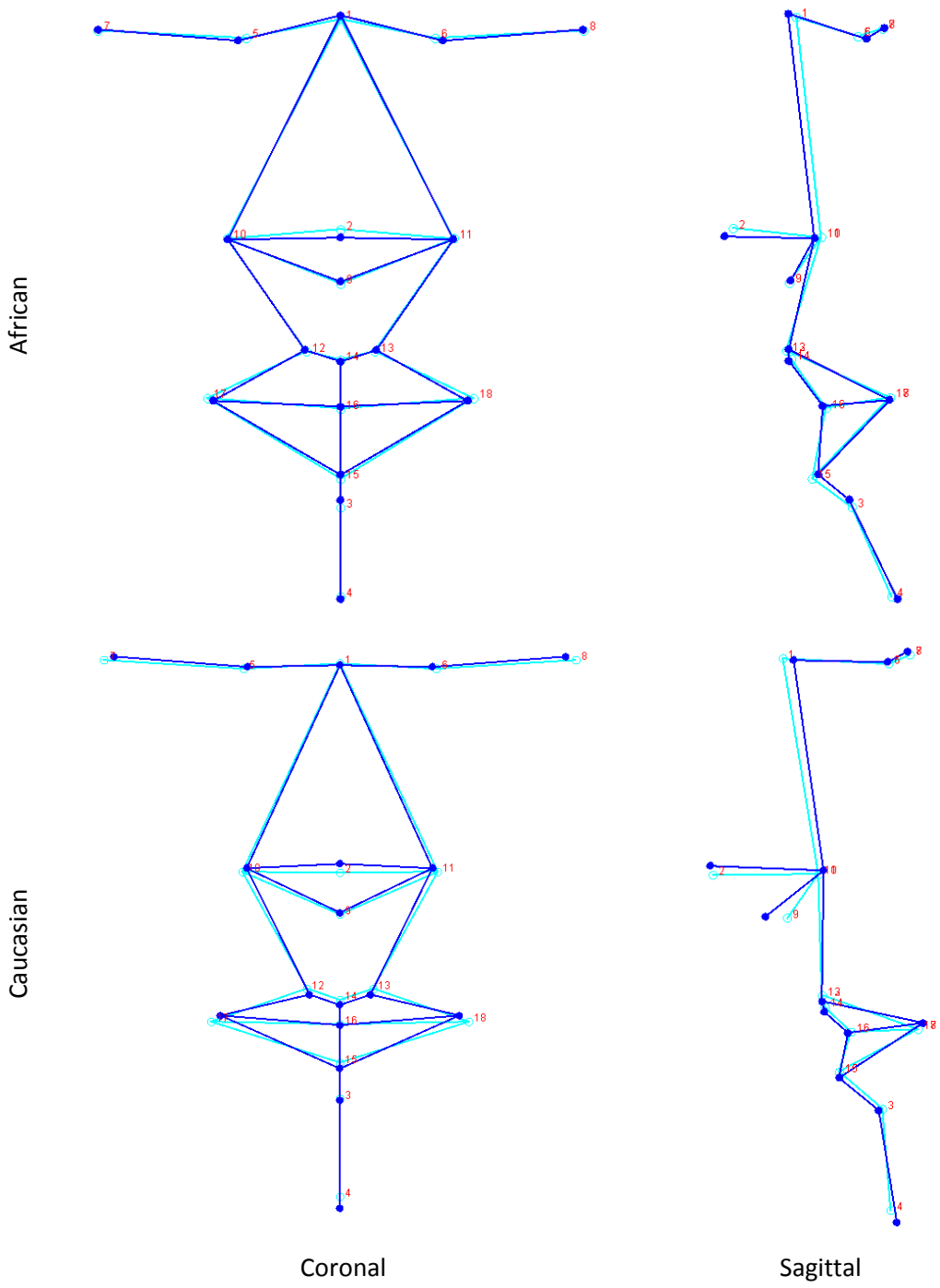


**Figure 7.3: Graphical illustrations of the mean shape difference between control (light blue) and schizophrenia (dark blue) cohorts for the male group.**

Qualitative assessment of the above graphs suggests that dysmorphology is more prominent in the nose and mouth regions, but possibly only in the Caucasian group. The down-turned appearance of the nose and posteriorly set subnasale in the male Caucasian schizophrenia group is consistent with the findings of Hennessy et al. (2010).

Table 7.3 below gives the Hotelling's $T^2$ distribution and parametric p-values for the male African and Caucasian, symmetric and asymmetric covariance matrices. No statistically significant differences in mean shape were found in either group between control and schizophrenia cohorts.

| | African | Caucasian |
|---|---|---|
| $T^2$ | 13.6458 | 9.9809 |
| p-value | 0.9990 | 0.9949 |

**Table 7.3: Hotelling's $T^2$ distribution and parametric p-values for the different cohorts**

### 7.2.2 Feature Selection

Feature set evaluation was carried out on the imported principal component scores. For both the African and Caucasian cohorts, the criteria identified for feature selection were the sum of estimated Mahalanobis distances and the minimum of estimated Mahalanobis distances, as they scored equally.

Branch-and-bound and sequential floating feature selection procedures identified those features (principal components) that possess the greatest discriminatory power. Both feature selection methods yielded the same features, PCs 14 and 15 in the African cohort and PCs 8 and 10 in the Caucasian cohort. Figure 7.4 and Figure 7.5 below show the separation between the control (blue) and schizophrenia (red) groups as shown by PCs 14 and 15 and PCs 8 and 10 in the African and Caucasian groups respectively

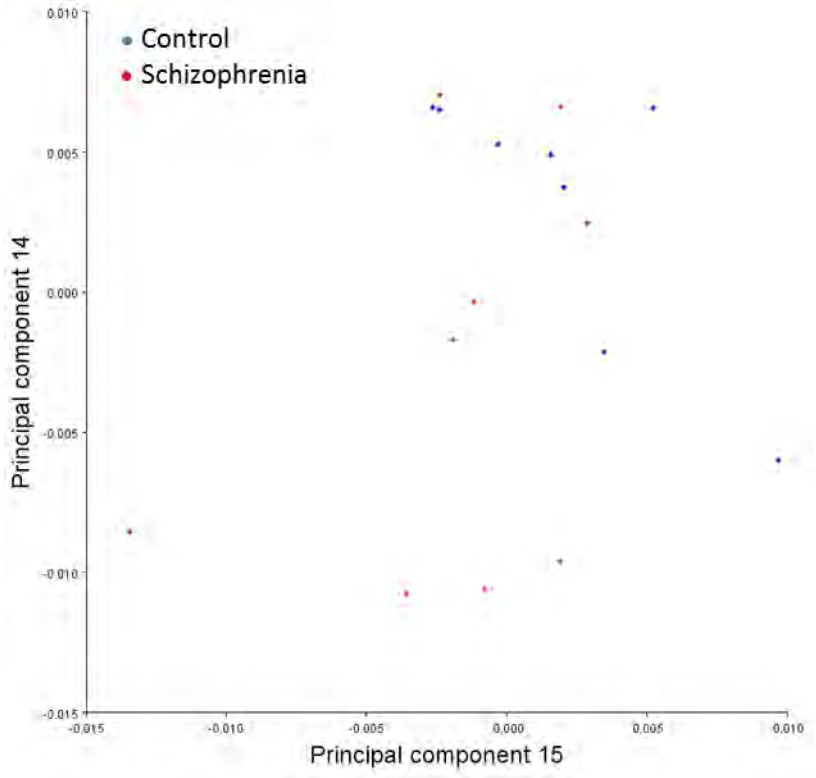


**Figure 7.4: Principal components 14 and 15 in the African cohort**

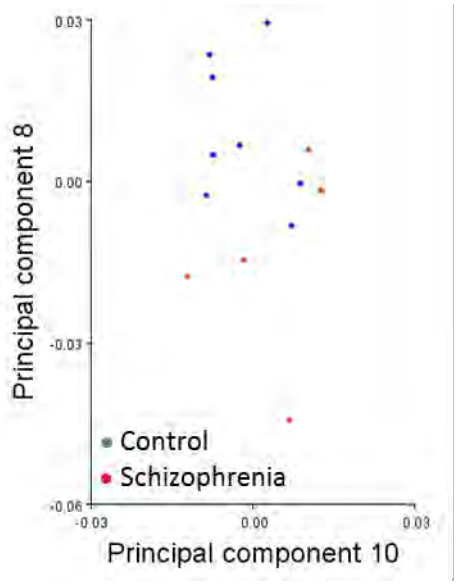


**Figure 7.5: Principal components 8 and 10 in the Caucasian cohort**

Figure 7.6 gives graphical representations of principal components 14 and 15 of the African cohort. These two PCs account for 0.5% and 0.27% of the shape variability respectively. The control group is shown with light blue lines and light blue landmarks, the schizophrenia group is shown with dark blue lines and solid dark blue landmarks and the shape differences have not been scaled.

Considering shape variation common to both PCs in the African cohort, there is an overall widening of the eyes (inner-to-outer canthi). The nose appears to be upturned (superior pronasale) and the mouth narrower (cheilion-to-cheilion). PC14 describes an anteroinferior displacement of the nasion, a posterior displacement of the alare and downturned mouth (cheilion-stomion-cheilion). PC15 describes an inward slanting of the eyes (inferior inner and superior outer canthi), a widening of the nose (alare-to-alare), inferior displacement of the alare and upturned mouth.

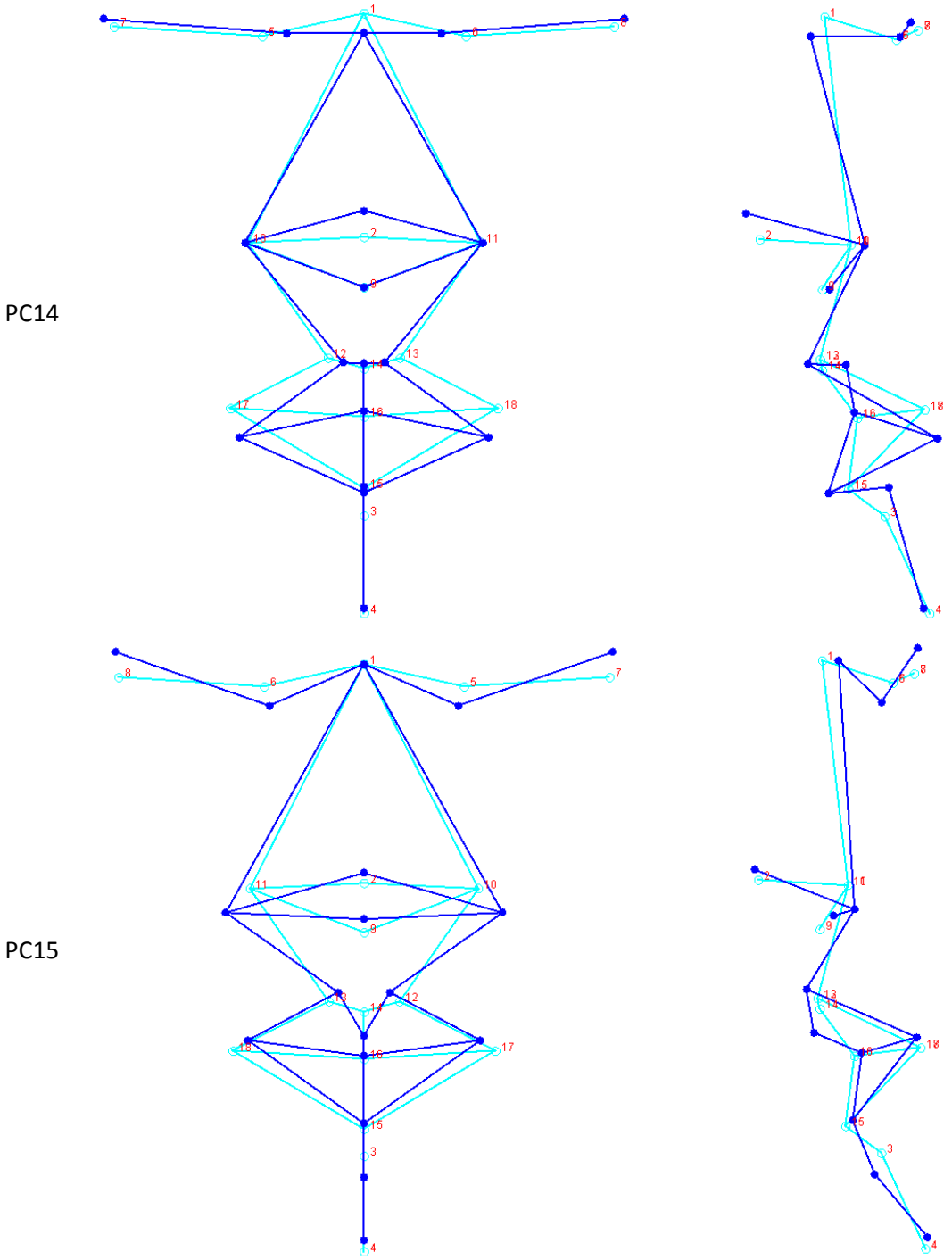


**Figure 7.6: Principal component 14 and 15 shape changes between control (light blue) and schizophrenia (dark blue) in the African group.**

Figure 7.7 shows the graphical representations of PCs 8 and 10 of the Caucasian cohort. These PCs contribute 3.12% and 0.88% respectively towards shape variability between the control and schizophrenia groups.

The PCs highlight an inferior setting of the eyes (inner and outer canthi), anteriorly set alare and downturned mouth (cheilion-stomion-cheilion). PC8 describes an anteriorly set nasion and downturned nose (inferior pronasale). PC10 describes a superoinferiorly displaced nasion, a slightly upturned or superiorly set nose (superior pronasale) and a chin that is posteriorly set (posterior pogonion).

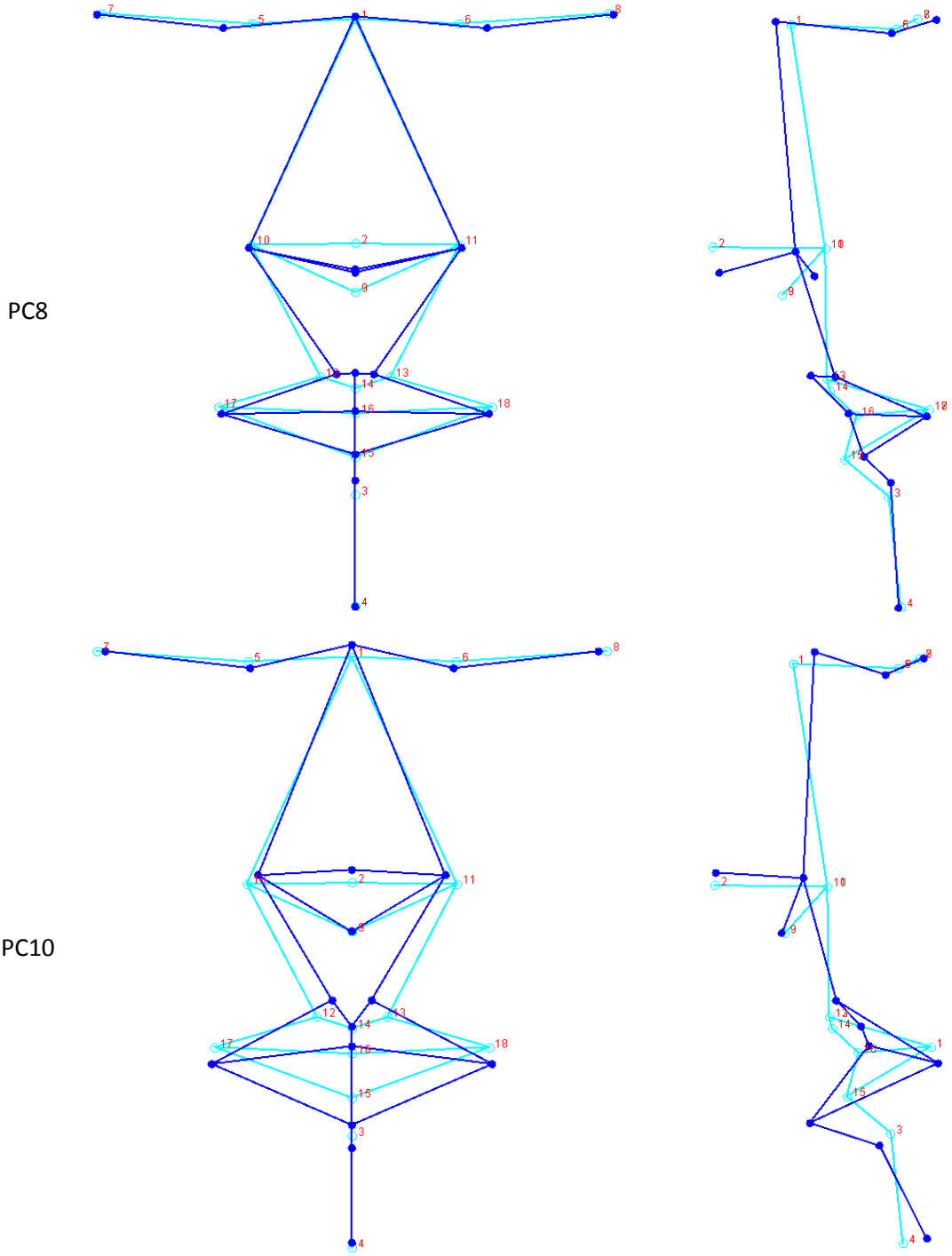


**Figure 7.7: Principal component 8 and 10 shape changes between control (light blue) and schizophrenia (dark blue) in the Caucasian group.**

### 7.2.3 Classification Accuracy

Leave-one-out cross-validation was carried out on the PC scores prior to and after feature selection to investigate the effect of feature selection on classification accuracy. The cross-validation prior to feature selection identified the quadratic Bayes normal classifier as the most accurate classifier for the African cohort. After feature selection, the nearest mean classifier best separated the control and schizophrenia groups. Results of leave-one-out cross-validation for the African cohort are shown in Table 7.4.

| | **Prior to feature selection** | **After feature selection** |
|---|---|---|
| Normal mean classifier | 29.4% | 70.6% |
| Logistic linear classifier | 23.5% | 64.7% |
| Support vector machine with RBF | 41.2% | 23.5% |
| Quadratic Bayes normal classifier | 76.5% | 64.7% |
| k-nearest neighbour classifier | 52.9% | 64.7% |
| Average | 44.7% | 58.6% |

**Table 7.4: Classification accuracy via leave-one-out cross-validation for the African cohort.**

The k-nearest neighbour classifier performed the best in separating the control and schizophrenia groups in the Caucasian cohort both before and after feature selection. Results of leave-one-out cross-validation for the Caucasian cohort are shown in Table 7.5.

| | **Prior to feature selection** | **After feature selection** |
|---|---|---|
| Normal mean classifier | 7.7% | 69.9% |
| Logistic linear classifier | 23.1% | 61.5% |
| Support vector machine with RBF | 61.5% | 61.5% |
| Quadratic Bayes normal classifier | 38.5% | 46.1% |
| k-nearest neighbour classifier | 61.5% | 76.9% |
| Average | 38.5% | 63.1% |

**Table 7.5: Classification accuracy via leave-one-out cross-validation for the Caucasian cohort.**

## 7.3 Discussion

Using the stereophotogrammetry system, those principal components exhibiting greatest discriminatory power were positively identified using feature selection techniques. These principal components exhibited craniofacial differences consistent with previous findings. Leave-one-out

cross-validation demonstrated that, to a certain degree of accuracy, classification can assign the objects in the dataset to their classes.

### 7.3.1 Shape Differences

The use of discriminant function analysis, in this application a Fisher's based algorithm, did not find statistically significant features between the groups.

However, visual examination of those features (PCs) possessing greatest discriminatory power did show shape variation between healthy control and schizophrenia cohorts in male African and Caucasian groups. The shape differences are summarised in Table 7.6 below.

| | **African** | **Caucasian** |
|---|---|---|
| Eyes | • Wider<br>• Inward slanting (cat-like) | • Narrower<br>• Wider apart |
| Nose | • Wider<br>• Upturned | • Narrower<br>• Downturned<br>• Anteriorly set at base<br>• Posteriorly set nasion |
| Mouth | • Narrower<br>• Downturned | • Wider<br>• Downturned<br>• Posteriorly set<br>• Thicker lips |
| Chin | | • Posteriorly set |

**Table 7.6: Summary of shape changes in African and Caucasian schizophrenia patients**

Unfortunately, very little prior work has explored craniofacial dysmorphology in the African population. One set of researchers found significant differences in the overall height of the male African face, claiming a shorter overall length in the schizophrenia group (Compton et al., 2007). This study was not able to reproduce this result, however other shape differences are described.

Hennessy et al. (2007) performed arguably the most comprehensive phenotypic characterisation of the male Caucasian schizophrenic. Some shape changes from the present study are in agreement with this previous work. These are a downturned nose as reported by principal component 8 and posteriorly set nasion, and posteriorly set mouth and chin as reported by principal component 10.

The comparative findings in this study to previous work are encouraging as they demonstrate the potential of the stereophotogrammetry system for this purpose. That the study groups are quite small must be considered when describing shape variation. While this study recruited 17 African participants (8 control, 9 schizophrenia) and 13 Caucasian participants (8 control, 5 schizophrenia), Compton et al. (2007) and Hennessy et al. (2007) recruited 77 participants (35 control, 42 schizophrenia) and 95 participants (37 control, 58 schizophrenia) respectively. However,

Mutsvangwa et al. (2010) found statistically significant shape variation in children with foetal alcohol syndrome (FAS) with 5- and 12-year-old groups with 15 (11 control, 4 FAS) and 19 (6 control, 13 FAS) study participants respectively.

The fact that the shape difference is described by lower-order PCs must also be considered. Lower-order PCs may represent noise in the data and as such interpretation of the shape change described by these PCs may not truly reflect the shape change (if any exists) between groups.

### 7.3.2 Feature Selection and Classification Accuracy

Feature selection was applied to identify those features with the greatest discriminatory power between the groups. The features identified accounted for less than 1% of shape variability in the African cohort and 4% of shape variability in the Caucasian cohort. This suggests that the hypothesised dysmorphology in schizophrenia is subtle.

The findings from the leave-one-out cross-validation illustrated the need for a classifier tailored to the data presented. In the African group, the validation identified the normal mean classifier as the best suited classifier, achieving 71% classification accuracy. The best suited classifier in the Caucasian group proved to be the k-nearest neighbour classifier, achieving 77% classification accuracy. This is comparable to Mutsvangwa (2009) who reported best-case 87% and 79% classification accuracy in five- and twelve-year-old children with foetal alcohol syndrome, respectively.

Additionally, leave-one-out cross-validation highlighted the benefit of feature selection to produce a subset for optimised classification. In the African cohort, the average classification accuracy prior to feature selection was 45%. The average classification accuracy improved to 58% after feature selection. The improvement in classification accuracy was more noticeable in the Caucasian cohort, with average classification accuracy improving from 38% before feature selection to 63% after feature selection.

The findings from feature selection, classification evaluation and visualisation of craniofacial variability between the groups must be viewed conservatively, however the classification accuracy achieved given this small sample is encouraging. The scope of this project was to evaluate the efficacy of a stereophotogrammetry system to detect craniofacial dysmorphology in schizophrenia. This has been achieved even with this small sample size. Further data should be collected to support this as well as further investigate the schizophrenia phenotype. The characterisation provided in this study is merely hypothetical at this stage, as it must be considered that a study sample of this size may not be sufficient to discriminate between true variation between the groups and inherent

variability in face shape. A larger study cohort will improve the confidence of the characterisation not only of the phenotypic shape, but may also be able to identify and discriminate any potential outliers.

# 8. Discussion, Conclusion and Recommendations

This project sought to test the efficacy of a stereophotogrammetry system to detect craniofacial dysmorphology in schizophrenia patients in an attempt to find a cost-effective alternative to the state-of-the-art 3D laser scanning technology. In South Africa, budgeting priorities in healthcare lie with HIV/AIDS and tuberculosis. Investigations into the cost of a local commercially available 3D laser scanner (Creaform Go!SCAN 3D, www.hmrhightech.co.za) found the cost to be in excess of R250,000 excluding VAT (quoted June 2013). The system used in this project would not exceed R40,000. The development of a low-cost system could create an imaging-based anthropometric tool more accessible to developing countries, which to date seem to have utilised direct anthropometry.

Several previous studies have successfully identified dysmorphology in schizophrenia using both direct (Lane et al., 1997; Trixler, Tényi, Csábi, & Szabó, 2001) and indirect (Hennessy et al., 2004, 2007) anthropometric methods, and the goal of this study was to determine whether the findings using a stereophotogrammetry system would agree with the results of these previous studies.

## 8.1 Efficacy of the Stereophotogrammetry System

The system used in this study was successfully implemented in the detection of craniofacial dysmorphology in schizophrenia, and described dysmorphology within a Caucasian population consistent with that described previously (Hennessy et al., 2004, 2007). The system performed better in classification of the Caucasian cohort than the African cohort. This could be attributed to difficulty in landmark mapping using images of subjects with darker skin tone. Alternatively, the presentation of craniofacial dysmorphology in the African population could be more subtle than that in the Caucasian population. Previous studies investigating craniofacial dysmorphology in schizophrenia in an African cohort (Compton et al., 2007) did not report dysmorphology in as much detail as studies investigating the same in a Caucasian cohort. However, the studies did not use the same measurement modalities. With regard to the present study, given the small sample sizes, conclusions about the relative classification accuracy in the two cohorts cannot be drawn with great confidence.

The detection of shape variation and its characterisation in line with previous studies demonstrate the efficacy of a simple stereophotogrammetry system for the detection of craniofacial dysmorphology in schizophrenia

## 8.2 Study Limitations

Data collection, landmark visualisation and questions of precision and reliability are all areas that should be addressed should further studies be carried out using the stereophotogrammetry system used in this project.

### 8.2.1 Data Collection and Sample Size

The rate of data collection was extremely slow (data were collected over a three-year period), limiting the number of participants per group. Consequently the sample size was small which may call into question the strength of the findings of this study. The small sample size, and the associated potential sampling error, may have greatly inhibited the study's ability to characterise dysmorphology in the schizophrenia groups.

### 8.2.2 Camera Rig and Landmark Visualisation

Previous studies in craniofacial dysmorphology in schizophrenia report measurements of facial width (Compton et al., 2007; Hennessy et al., 2007, 2010) and statistically significant shape differences in this region (tragion-to-tragion). With the current camera rig, the images acquired do not show enough of an oblique view of the subject's face to visualise the tragion and hence no facial width measurements could be carried out.

### 8.2.3 Landmark Mapping

Accuracy of manual landmark mapping is a potential source of error. A "point-and-click" method is used to manually place markers at what the operator best identifies as those craniofacial landmarks chosen for analysis. This is a subjective procedure and has the potential for significant study error. Compounding the problem are the soft tissue landmarks, those landmarks not falling on any easily identifiable feature of the craniofacial region.

In Section 4.2.1.1, the use of three cameras for landmark error minimisation is discussed. The same argument illustrates the potential for error in both accuracy and precision in landmark mapping. The triangulation of each landmark in 3D space is heavily reliant on the accurate positioning of the initial landmark in the first of the three images for each subject. If that initial landmark is erroneously placed, the accuracy of that landmark is compromised. Also, if each landmark is not identified similarly between subjects, this can result in imprecise landmark configurations which jeopardises the outcomes of the subsequent analytical procedures.

## 8.3 Conclusion

A stereophotogrammetry tool very similar to the one used in this project has been successfully implemented for the identification and characterisation of craniofacial dysmorphology in foetal alcohol syndrome (Mutsvangwa, 2009).

This study suggests that such a tool has potential in the identification of craniofacial dysmorphology in schizophrenia in African and Caucasian populations. For the Caucasian cohort, this study characterised dysmorphology consistent with the literature. However, the small sample size necessitates caution in drawing conclusions from the study.

The stereophotogrammetry system in this study (and one of similar design) has now been successfully implemented in the characterisation of craniofacial dysmorphology in schizophrenia and foetal alcohol syndrome (Mutsvangwa et al., 2009, 2010). A sound system has been developed and tested that could now form the basis for future studies.

## 8.4 Recommendations

To optimise and streamline further studies implementing a stereophotogrammetry system such as the system used in this study, the following should be considered.

The addition of fourth and fifth oblique cameras could aid in the visualisation and identification of data that otherwise cannot be obtained.

The subjectivity of the landmark process must not be underestimated and is a potential pitfall for any study. Landmark mapping must therefore be done by those who have thorough understanding of the craniofacial morphology.

A larger study with more participants is recommended to confirm the findings, and also to gain a deeper understanding of craniofacial dysmorphology associated with Schizophrenia in Africans, a group in which little related work has been done to date.

A similar study could be done in bipolar disorder. Hennesy et al. (2010) characterised craniofacial dysmorphology in bipolar disorder. It could be investigated whether the stereophotogrammetry system used in the current study is able to detect and characterise shape change in bipolar disorder.

## References


Aldridge, K., George, I. D., Cole, K. K., Austin, J. R., Takahashi, T. N., Duan, Y., & Miles, J. H. (2011). Facial phenotypes in subgroups of prepubertal boys with autism spectrum disorders are correlated with clinical phenotypes. *Molecular Autism*, *2*(1), 15. doi:10.1186/2040-2392-2-15

Allanson, J. E. (1997). Objective techniques for craniofacial assessment: what are the choices? *American Journal of Medical Genetics*, *70*(1), 1–5.

Aung, S. C., Ngim, R. C. K., & Lee, S. T. (1995). Evaluation of the laser scanner as a surface measuring tool and its accuracy compared with direct facial anthropometric measurements. *British Journal of Plastic Surgery*, *48*(8), 551–558. doi:10.1016/0007-1226(95)90043-8

Bookstein, F. L. (1991). *Morphometric tools for landmark data: geometry and biology*. *Cambridge University Press* (Vol. 10). New York: Cambridge University Press. doi:10.1017/CBO9780511573064

Buckley, P. F., Dean, D., Bookstein, F. L., Friedman, L., Kwon, D., Lewin, J. S., … Lys, C. (1999). Three-dimensional magnetic resonance-based morphometrics and ventricular dysmorphology in schizophrenia. *Biological Psychiatry*, *45*(1), 62–67. doi:10.1016/S0006-3223(98)00067-5

Buckley, P. F., Dean, D., Bookstein, F. L., Han, S., Yerukhimovich, M., Min, K.-J., & Singer, B. (2005). A three-dimensional morphometric study of craniofacial shape in schizophrenia. *The American Journal of Psychiatry*, *162*(3), 606–8. doi:10.1176/appi.ajp.162.3.606

Compton, M. T., Brudno, J., Kryda, A. D., Bollini, A. M., & Walker, E. F. (2007). Facial measurement differences between patients with schizophrenia and non-psychiatric controls. *Schizophrenia Research*, *93*(1-3), 245–52. doi:10.1016/j.schres.2007.03.017

Dash, M., & Liu, H. (1997). Feature selection for classification. *Intelligent Data Analysis*, *1*(1-4), 131–156. doi:10.1016/S1088-467X(97)00008-5

Douglas, T. S. (2004). Image processing for craniofacial landmark identification and measurement: a review of photogrammetry and cephalometry. *Computerized Medical Imaging and Graphics : The Official Journal of the Computerized Medical Imaging Society*, *28*(7), 401–9.

Douglas, T. S., & Mutsvangwa, T. E. M. (2010). A review of facial image analysis for delineation of the facial phenotype associated with fetal alcohol syndrome. *American Journal of Medical Genetics. Part A*, *152A*(2), 528–36.

Duda, R. O., Hart, P. E., & Stork, D. G. (2000). Pattern Classification (2nd Edition). Retrieved from http://dl.acm.org/citation.cfm?id=954544

Duin, R. P. W., Juszczak, P., Paclik, P., Pekalska, E., de Ridder, D., Tax, D. M. J., & Verzakov, S. (2007). *PRTools 4.1, Matlab Toolbox for Pattern Recognition*. Delft University of Technology.

Fakhroddin, M., Ahmad, G., & Imran, S. (2014). Morphometric characteristics of craniofacial features in patients with schizophrenia. *Journal of Psychiatry*, *17*, 514–519. Retrieved from http://omicsonline.com/open-

access/morphometric_characteristics_of_craniofacial_features_in_patients_with_schizophrenia.pdf?aid=24010

Fang, F., Clapham, P. J., & Chung, K. C. (2011). A systematic review of interethnic variability in facial dimensions. *Plastic and Reconstructive Surgery*, *127*(2), 874–81. doi:10.1097/PRS.0b013e318200afdb

Farkas, L. G. (1994). *Anthropometry of the Head and Face* (2nd ed.). New York: Raven Press.

Farkas, L. G., & Deutsch, C. K. (1996). Anthropometric determination of craniofacial morphology. *American Journal of Medical Genetics*, *65*(1), 1–4.

Farkas, L. G., Katic, M. J., & Forrest, C. R. (2007). Comparison of craniofacial measurements of young adult African-American and North American white males and females. *Annals of Plastic Surgery*, *59*(6), 692–8. doi:10.1097/01.sap.0000258954.55068.b4

Farkas, L. G., Katic, M. J., Forrest, C. R., Alt, K. W., Bagic, I., Baltadjiev, G., … Yahia, E. (2005). International anthropometric study of facial morphology in various ethnic groups/races. *The Journal of Craniofacial Surgery*, *16*(4), 615–46. Retrieved from http://www.ncbi.nlm.nih.gov/pubmed/16077306

Garson, G. D. (2012). Discriminant Function Analysis. Retrieved from http://www.statisticalassociates.com/discriminantfunctionanalysis.htm

Green, M. F., Satz, P., Gaier, D. J., Ganzell, S., & Kharabi, F. (1989). Minor physical anomalies in schizophrenia. *Schizophrenia Bulletin*, *15*(1), 91–9.

Guy, J. D., Majorski, L. V, Wallace, C. J., & Guy, M. P. (1983). The incidence of minor physical anomalies in adult male schizophrenics. *Schizophrenia Bulletin*, *9*(4), 571–82.

Halazonetis, D. J. (2004). Morphometrics for cephalometric diagnosis. *American Journal of Orthodontics and Dentofacial Orthopedics : Official Publication of the American Association of Orthodontists, Its Constituent Societies, and the American Board of Orthodontics*, *125*(5), 571–81. doi:10.1016/S0889540604000319

Hennessy, R. J., Baldwin, P. A., Browne, D. J., Kinsella, A., & Waddington, J. L. (2007). Three-dimensional laser surface imaging and geometric morphometrics resolve frontonasal dysmorphology in schizophrenia. *Biological Psychiatry*, *61*(10), 1187–94.

Hennessy, R. J., Baldwin, P. A., Browne, D. J., Kinsella, A., & Waddington, J. L. (2010). Frontonasal dysmorphology in bipolar disorder by 3D laser surface imaging and geometric morphometrics: comparisons with schizophrenia. *Schizophrenia Research*, *122*(1-3), 63–71.

Hennessy, R. J., Kinsella, A., & Waddington, J. L. (2002). 3D laser surface scanning and geometric morphometric analysis of craniofacial shape as an index of cerebro-craniofacial morphogenesis: initial application to sexual dimorphism. *Biological Psychiatry*, *51*(6), 507–14.

Hennessy, R. J., Lane, A., Kinsella, A., Larkin, C., O'Callaghan, E., & Waddington, J. L. (2004). 3D morphometrics of craniofacial dysmorphology reveals sex-specific asymmetries in schizophrenia. *Schizophrenia Research*, *67*(2-3), 261–8.

Hennessy, R. J., & Stringer, C. B. (2002). Geometric morphometric study of the regional variation of modern human craniofacial form. *American Journal of Physical Anthropology*, *117*(1), 37–48. doi:10.1002/ajpa.10005

Jain, A., & Zongker, D. (1997). Feature selection: evaluation, application, and small sample performance. *IEEE Transactions on Pattern Analysis and Machine Intelligence*, *19*(2), 153–158. doi:10.1109/34.574797

JCGM. (2012). *International vocabulary of metrology - Basic and general concepts and associated terms (VIM)* (No. 200:2012) (3rd Editio.). Joint Committee for Guides in Metrology.

Jolliffe, I. T. (2002). *Principal component analysis* (2nd ed.). Springer. Retrieved from http://books.google.com/books?hl=en&lr=&id=_olByCrhjwIC&pgis=1

Kittler, J. (1986). Feature selection and extraction. In *Handbook of pattern recognition and image processing* (pp. 59–83). New York: Academic Press.

Klingenberg, C. P. (2011). MorphoJ: an integrated software package for geometric morphometrics. *Molecular Ecology Resources*, *11*(2), 353–357.

Lane, A., Kinsella, A., Murphy, P., Byrne, M., Keenan, J., Colgan, K., … O'Callaghan, E. (1997). The anthropometric assessment of dysmorphic features in schizophrenia as an index of its developmental origins. *Psychological Medicine*, *27*(05), 1155–1164.

Lin, A.-S., Chang, S.-S., Lin, S.-H., Peng, Y.-C., Hwu, H.-G., & Chen, W. J. (2014). Minor physical anomalies and craniofacial measures in patients with treatment-resistant schizophrenia. *Psychological Medicine*, 1–12. doi:10.1017/S0033291714002931

Lohr, J. B., & Flynn, K. (1993). Minor physical anomalies in schizophrenia and mood disorders. *Schizophrenia Bulletin*, *19*(3), 551–6.

Luhmann, T., Robson, S., Kyle, S., & Harley, I. (2006, May 17). Close Range Photogrammetry: Principles, Methods and Applications. Whittles. Retrieved from http://discovery.ucl.ac.uk/1393597/

Majid, Z., Chong, A. K., Ahmad, A., Setan, H., & Samsudin, A. R. (2005). Photogrammetry and 3D laser scanning as spatial data capture techniques for a national craniofacial database. *The Photogrammetric Record*, *20*(109), 48–68.

Meintjes, E. M., Douglas, T. S., Martinez, F., Vaughan, C. L., Adams, L. P., Stekhoven, A., & Viljoen, D. (2002). A stereo-photogrammetric method to measure the facial dysmorphology of children in the diagnosis of fetal alcohol syndrome. *Medical Engineering & Physics*, *24*(10), 683–689. doi:10.1016/S1350-4533(02)00114-5

Mitteroecker, P., & Gunz, P. (2009). Advances in Geometric Morphometrics. *Evolutionary Biology*, *36*(2), 235–247.

Murray, R. M., & Lewis, S. W. (1987). Is schizophrenia a neurodevelopmental disorder? *British Medical Journal*, *295*(6600), 681–2.

Mutsvangwa, T. E. M. (2006). *Statistical analysis of facial landmark data for optimisation of Fetal Alcohol Syndrome diagnosis*. University of Cape Town.

Mutsvangwa, T. E. M. (2009). *Characterization of the facial phenotype associated with fetal alcohol syndrome using stereo-photogrammetry and geometric morphometrics*. University of Cape Town.

Mutsvangwa, T. E. M., & Douglas, T. S. (2007). Morphometric analysis of facial landmark data to characterize the facial phenotype associated with fetal alcohol syndrome. *Journal of Anatomy*, *210*(2), 209–220.

Mutsvangwa, T. E. M., Meintjes, E. M., Viljoen, D. L., & Douglas, T. S. (2010). Morphometric analysis and classification of the facial phenotype associated with fetal alcohol syndrome in 5- and 12-year-old children. *American Journal of Medical Genetics. Part A*, *152A*(1), 32–41.

Mutsvangwa, T. E. M., Smit, J., Hoyme, H. E., Kalberg, W., Viljoen, D. L., Meintjes, E. M., & Douglas, T. S. (2009). Design, construction, and testing of a stereo-photogrammetric tool for the diagnosis of fetal alcohol syndrome in infants. *IEEE Transactions on Medical Imaging*, *28*(9), 1448–58.

Narendra, P. M., & Fukunaga, K. (1977). A Branch and Bound Algorithm for Feature Subset Selection. *IEEE Transactions on Computers*, *C-26*(9), 917–922. doi:10.1109/TC.1977.1674939

Obafemi-Ajayi, T., Miles, J. H., Takahashi, T. N., Qi, W., Aldridge, K., Zhang, M., … Duan, Y. (2014). Facial Structure Analysis Separates Autism Spectrum Disorders into Meaningful Clinical Subgroups. *Journal of Autism and Developmental Disorders*. doi:10.1007/s10803-014-2290-8

Photometrix. (2004). Australis Users Manual. PO Box 3023, Kew, Vic 3101, Australia: Photometrix Pty Ltd. Retrieved from http://www.photometrix.com.au/downloads/australis/AustralisGuide.pdf

Photometrix. (2007). User Manual for Australis. PO Box 3023, Kew, Vic 3101, Australia: Photometrix Pty Ltd.

Pudil, P., Ferri, F. J., Novovicova, J., & Kittler, J. (1994). Floating search methods for feature selection with nonmonotonic criterion functions. In *Proceedings of the 12th IAPR International Conference on Pattern Recognition (Cat. No.94CH3440-5)* (Vol. 2, pp. 279–283). IEEE Comput. Soc. Press. doi:10.1109/ICPR.1994.576920

Ramos, S. D. S., & Rickard Liow, S. J. (2013). Discriminant Function Analysis. In C. A. Chapelle (Ed.), *The Encyclopedia of Applied Linguistics*. Blackwell Publishing Ltd. doi:10.1002/9781405198431.wbeal0335

Rapoport, J. L., Addington, A. M., Frangou, S., & Psych, M. R. C. (2005). The neurodevelopmental model of schizophrenia: update 2005. *Molecular Psychiatry*, *10*(5), 434–49.

Robinson, D. L., Blackwell, P. G., Stillman, E. C., & Brook, A. H. (2001). Planar Procrustes analysis of tooth shape. *Archives of Oral Biology*, *46*(3), 191–199. doi:10.1016/S0003-9969(00)00120-5

Roelofse, M. M., Steyn, M., & Becker, P. J. (2008). Photo identification: facial metrical and morphological features in South African males. *Forensic Science International*, *177*(2-3), 168–75. doi:10.1016/j.forsciint.2007.12.003

Rohlf, F. J. (1999). Shape Statistics: Procrustes Superimpositions and Tangent Spaces. *Journal of Classification*, *16*(2), 197–223.

Smith, L. I. (2002). A tutorial on Principal Component Analysis. Retrieved May 10, 2011, from http://staf.cs.ui.ac.id/WebKuliah/citra/2004/principal_components.pdf

Stegmann, M., & Gomez, D. (2002). A brief introduction to statistical shape analysis.

Trixler, M., Tényi, T., Csábi, G., & Szabó, R. (2001). Minor physical anomalies in schizophrenia and bipolar affective disorder. *Schizophrenia Research*, *52*(3), 195–201.

Van der Heijden, F., Duin, R. P. W., de Ridder, D., & Tax, D. M. J. (2005). *Classification, parameter estimation and state estimation: an engineering approach using matlab*. John Wiley & Sons, Ltd. Retrieved from http://eprints.eemcs.utwente.nl/17475/

Van Os, J., & Kapur, S. (2009). Schizophrenia. *Lancet*, *374*(9690), 635–645.

Waddington, J. L., Lane, A., Larkin, C., & O'Callaghan, E. (1999). The neurodevelopmental basis of schizophrenia: clinical clues from cerebro-craniofacial dysmorphogenesis, and the roots of a lifetime trajectory of disease. *Biological Psychiatry*, *46*(1), 31–9.

Waldrop, M. F., Pedersen, F. A., & Bell, R. Q. (1968). Minor physical anomalies and behavior in preschool children. *Child Development*, *39*(2), 391–400.

Webb, A. R., & Copsey, K. D. (2011). *Statistical Pattern Recognition* (Third Edit.). John Wiley & Sons, Ltd. Retrieved from http://books.google.es/books/about/Statistical_Pattern_Recognition.html?hl=es&id=WpV9Xt-h3O0C&pgis=1

Weinberg, S. M., Jenkins, E. A., Marazita, M. L., & Maher, B. S. (2007). Minor physical anomalies in schizophrenia: a meta-analysis. *Schizophrenia Research*, *89*(1-3), 72–85. doi:10.1016/j.schres.2006.09.002

Weinberg, S. M., Scott, N. M., Neiswanger, K., Brandon, C. A., & Marazita, M. L. (2004). Digital three-dimensional photogrammetry: evaluation of anthropometric precision and accuracy using a Genex 3D camera system. *The Cleft Palate-Craniofacial Journal : Official Publication of the American Cleft Palate-Craniofacial Association*, *41*(5), 507–18. doi:10.1597/03-066.1

Wong, J. Y., Oh, A. K., Ohta, E., Hunt, A. T., Rogers, G. F., Mulliken, J. B., & Deutsch, C. K. (2008). Validity and reliability of craniofacial anthropometric measurement of 3D digital photogrammetric images. *The Cleft Palate-Craniofacial Journal : Official Publication of the American Cleft Palate-Craniofacial Association*, *45*(3), 232–9. doi:10.1597/06-175

Zhao, Q., Rosenbaum, K., Okada, K., Zand, D. J., Sze, R., Summar, M., & Linguraru, M. G. (2013). Automated Down syndrome detection using facial photographs. *Conference Proceedings : ... Annual International Conference of the IEEE Engineering in Medicine and Biology Society. IEEE Engineering in Medicine and Biology Society. Annual Conference*, *2013*, 3670–3. doi:10.1109/EMBC.2013.6610339

## Appendix A – Precision and Reliability Tests

| Measurement | Stereophotogrammetry | | | Direct Anthropometry | | |
|---|---|---|---|---|---|---|
| | Grandmean (mm) | REM (%) | Rating | Grandmean (mm) | REM (%) | Rating |
| **Operator 1** | | | | | | |
| n –al | 52.84 | 0.45 | Excellent | 52.62 | 0.11 | Excellent |
| prn – al | 33.39 | 0.68 | Excellent | 33.47 | 1.23 | Very good |
| al – cph | 26.12 | 0.32 | Excellent | 25.95 | 1.19 | Very good |
| cph – ch | 28.57 | 0.92 | Excellent | 27.78 | 0.07 | Excellent |
| ch – pg | 43.56 | 0.75 | Excellent | 38.84 | 0.23 | Excellent |
| n – pg | 114.70 | 0.12 | Excellent | 113.59 | 1.12 | Very good |
| cph – cph | 15.89 | 2.97 | Very good | 14.76 | 0.81 | Excellent |
| **Operator 2** | | | | | | |
| n –al | 52.21 | 1.67 | Very good | 52.16 | 2.20 | Very good |
| prn – al | 32.07 | 3.21 | Very good | 32.57 | 3.10 | Very good |
| al – cph | 25.74 | 2.64 | Very good | 25.04 | 4.91 | Good |
| cph – ch | 28.20 | 1.7 | Very good | 27.33 | 5.82 | Good |
| ch – pg | 43.39 | 0.00 | Excellent | 38.18 | 4.66 | Good |
| n – pg | 114.81 | 0.31 | Excellent | 110.99 | 0.86 | Excellent |
| cph – cph | 15.63 | 6.35 | Good | 13.60 | 7.58 | Moderate |

**Table A. 1: Intra-operator precision for operators 1 and 2**

| Measurement | Averaged measurements (mm) | | Grandmean (mm) | REM (%) | Rating |
|---|---|---|---|---|---|
| | Operator 1 | Operator 2 | | | |
| **Stereophotogrammetry** | | | | | |
| n –al | 52.84 | 52.21 | 52.53 | 1.20 | Very good |
| prn – al | 33.39 | 32.07 | 32.73 | 4.01 | Good |
| al – cph | 26.12 | 25.74 | 25.93 | 1.47 | Very good |
| cph – ch | 28.57 | 28.20 | 28.39 | 1.31 | Very good |
| ch – pg | 43.56 | 43.39 | 43.48 | 0.38 | Excellent |
| n – pg | 114.70 | 114.81 | 114.75 | 0.10 | Excellent |
| cph – cph | 15.89 | 15.63 | 15.76 | 1.65 | Very good |
| **Direct Anthropometry** | | | | | |
| n –al | 52.62 | 52.16 | 52.39 | 0.89 | Excellent |
| prn – al | 33.47 | 32.57 | 33.02 | 2.73 | Very good |
| al – cph | 25.95 | 25.04 | 25.49 | 3.57 | Very good |
| cph – ch | 27.78 | 27.33 | 27.55 | 1.65 | Very good |
| ch – pg | 38.84 | 38.18 | 38.51 | 1.70 | Very good |
| n – pg | 113.59 | 110.19 | 112.29 | 2.31 | Very good |
| cph – cph | 14.76 | 13.60 | 14.18 | 8.22 | Moderate |

**Table A. 2: Inter-operator precision for stereophotogrammetry and direct anthropometry.**

| Measurement | Averaged measurements (mm) Direct Anthropometry | Stereo-photogrammetry | Grandmean (mm) | REM (%) | Rating |
|---|---|---|---|---|---|
| **Operator 1** | | | | | |
| n –al | 52.62 | 52.84 | 52.73 | 0.43 | Excellent |
| prn – al | 33.47 | 33.39 | 33.43 | 0.24 | Excellent |
| al – cph | 25.95 | 26.12 | 26.03 | 0.67 | Excellent |
| cph – ch | 27.78 | 28.57 | 28.18 | 2.85 | Very good |
| ch – pg | 38.84 | 43.56 | 41.20 | 11.46 | Poor |
| n – pg | 113.59 | 114.70 | 114.14 | 0.97 | Excellent |
| cph – cph | 14.76 | 15.89 | 15.32 | 7.37 | Moderate |
| **Operator 2** | | | | | |
| n –al | 52.16 | 52.21 | 52.18 | 0.11 | Excellent |
| prn – al | 32.57 | 32.07 | 32.32 | 1.52 | Very good |
| al – cph | 25.04 | 25.74 | 25.39 | 2.76 | Very good |
| cph – ch | 27.33 | 28.20 | 27.76 | 3.16 | Very good |
| ch – pg | 38.18 | 43.39 | 40.79 | 12.78 | Poor |
| n – pg | 110.19 | 114.81 | 112.90 | 3.38 | Very good |
| cph – cph | 13.60 | 15.63 | 14.61 | 13.92 | Poor |

**Table A. 3: Normalised inter-modality reliability for operators 1 and 2 using the proportional error of magnitude method.**

# Appendix B – Principal Component and Feature Analysis

| | | PC1 | PC2 | PC3 | PC4 | PC5 | PC6 | PC7 | PC8 | PC9 | PC10 | PC11 | PC12 | PC13 | PC14 | PC15 |
|---|---|---|---|---|---|---|---|---|---|---|---|---|---|---|---|---|
| L1 | x1 | 0.050704 | 0.272969 | 0.155874 | -0.16871 | -0.30156 | -0.27295 | 0.033687 | -0.11727 | -0.05968 | 0.193128 | 0.233285 | -0.18407 | -0.02089 | -0.21076 | -0.00286 |
| | y1 | 0 | 0 | 0 | 0 | 0 | 0 | 0 | 0 | 0 | 0 | 0 | 0 | 0 | 0 | 0 |
| | z1 | 0.073634 | -0.38008 | 0.11032 | 0.126148 | 0.228913 | -0.05422 | 0.034216 | -0.03661 | -0.20983 | -0.17268 | 0.284154 | 0.132759 | -0.27955 | 0.149267 | -0.18033 |
| L2 | x2 | -0.08328 | 0.11563 | 0.218407 | -0.09468 | 0.194608 | 0.39639 | -0.00392 | -0.09814 | 0.258044 | 0.064549 | 0.213778 | 0.234178 | -0.07956 | 0.280788 | 0.113124 |
| | y2 | 0 | 0 | 0 | 0 | 0 | 0 | 0 | 0 | 0 | 0 | 0 | 0 | 0 | 0 | 0 |
| | z2 | -0.00443 | -0.17054 | 0.217465 | 0.527525 | -0.08558 | -0.33938 | 0.044797 | -0.06413 | 0.213214 | -0.04041 | 0.111899 | -0.34537 | 0.262018 | 0.149229 | 0.037534 |
| L3 | x3 | 0.019187 | 0.272775 | -0.21095 | 0.078044 | -0.04731 | -0.21538 | 0.181462 | -0.12199 | 0.112292 | -0.06426 | 0.185621 | 0.081902 | -0.24239 | 0.314526 | -0.23699 |
| | y3 | 0 | 0 | 0 | 0 | 0 | 0 | 0 | 0 | 0 | 0 | 0 | 0 | 0 | 0 | 0 |
| | z3 | -0.15819 | 0.042717 | -0.23179 | -0.06744 | 0.20776 | -0.18685 | -0.37212 | -0.0129 | 0.060677 | -0.10691 | 0.04355 | -0.27074 | -0.35922 | -0.04265 | 0.070113 |
| L4 | x4 | -0.12172 | 0.124589 | -0.02474 | 0.295264 | -0.04206 | 0.365916 | -0.033 | 0.222707 | -0.0559 | 0.13512 | 0.187409 | -0.4221 | -0.04804 | 0.056482 | 0.125204 |
| | y4 | 0 | 0 | 0 | 0 | 0 | 0 | 0 | 0 | 0 | 0 | 0 | 0 | 0 | 0 | 0 |
| | z4 | -0.4704 | -0.24951 | 0.275753 | -0.12499 | 0.068247 | -0.21032 | 0.256448 | 0.139073 | 0.04142 | 0.199365 | -0.20265 | 0.035054 | -0.10579 | 0.067534 | -0.02142 |
| L5 | x5 | 0.025658 | 0.038494 | -0.02496 | 0.123688 | -0.08869 | 0.041314 | 0.011642 | 0.159708 | -0.1427 | 0.088195 | -0.1437 | 0.017628 | 0.065799 | 0.028034 | -0.21276 |
| | y5 | 0.095352 | -0.02052 | -0.11248 | -0.05578 | 0.366988 | -0.04315 | 0.140855 | 0.017361 | 0.011645 | -0.04869 | 0.183498 | -0.04649 | 0.078456 | -0.26145 | -0.05729 |
| | z5 | -0.07138 | 0.085092 | 0.084962 | -0.29889 | -0.07197 | -0.05566 | -0.06531 | -0.19293 | 0.083849 | 0.077946 | 0.122031 | -0.06111 | 0.08317 | -0.03743 | 0.124934 |
| L6 | x6 | 0.025658 | 0.038494 | -0.02496 | 0.123688 | -0.08869 | 0.041314 | 0.011642 | 0.159708 | -0.1427 | 0.088195 | -0.1437 | 0.017628 | 0.065799 | 0.028034 | -0.21276 |
| | y6 | -0.09535 | 0.020524 | 0.112483 | 0.055777 | -0.36699 | 0.043151 | -0.14086 | -0.01736 | -0.01165 | 0.048692 | -0.1835 | 0.046488 | -0.07846 | 0.261451 | 0.057291 |
| | z6 | -0.07138 | 0.085092 | 0.084962 | -0.29889 | -0.07197 | -0.05566 | -0.06531 | -0.19293 | 0.083849 | 0.077946 | 0.122031 | -0.06111 | 0.08317 | -0.03743 | 0.124934 |
| L7 | x7 | 0.026824 | 0.06803 | 0.093995 | -0.05365 | 0.004032 | -0.06105 | 0.018821 | 0.204888 | 0.027011 | -0.26471 | -0.09623 | 0.06363 | -0.14 | 0.086921 | 0.278094 |
| | y7 | -0.00765 | -0.10512 | -0.28138 | -0.04052 | 0.09952 | 0.159086 | 0.161714 | -0.19795 | 0.047969 | 0.022001 | -0.1265 | -0.30883 | -0.08077 | 0.108864 | 0.032825 |
| | z7 | -0.06665 | 0.000117 | -0.1297 | -0.13211 | 0.019606 | 0.01086 | 0.037028 | 0.186357 | -0.08739 | 0.18645 | -0.22261 | -0.003 | -0.07002 | 0.080857 | -0.03637 |
| L8 | x8 | 0.026824 | 0.06803 | 0.093995 | -0.05365 | 0.004032 | -0.06105 | 0.018821 | 0.204888 | 0.027011 | -0.26471 | -0.09623 | 0.06363 | -0.14 | 0.086921 | 0.278094 |
| | y8 | 0.007654 | 0.105119 | 0.281375 | 0.040522 | -0.09952 | -0.15909 | -0.16171 | 0.197952 | -0.04797 | -0.022 | 0.126502 | 0.308826 | 0.080774 | -0.10886 | -0.03283 |
| | z8 | -0.06665 | 0.000117 | -0.1297 | -0.13211 | 0.019606 | 0.01086 | 0.037028 | 0.186357 | -0.08739 | 0.18645 | -0.22261 | -0.003 | -0.07002 | 0.080857 | -0.03637 |
| L9 | x9 | -0.01585 | 0.034521 | 0.24386 | 0.040426 | 0.238159 | 0.049464 | -0.0792 | -0.28501 | -0.28044 | -0.00892 | -0.05297 | 0.019532 | -0.06499 | 0.001137 | 0.146899 |
| | y9 | 0 | 0 | 0 | 0 | 0 | 0 | 0 | 0 | 0 | 0 | 0 | 0 | 0 | 0 | 0 |
| | z9 | -0.0149 | 0.034401 | 0.024174 | 0.108004 | -0.14774 | 0.103498 | -0.01092 | -0.04996 | 0.199966 | -0.15456 | -0.04116 | 0.167822 | -0.08624 | -0.07751 | -0.15056 |

**Table B.1: Male African cohort – Principal component coordinates (eigenvectors) using the symmetric covariance matrix**

| | | PC1 | PC2 | PC3 | PC4 | PC5 | PC6 | PC7 | PC8 | PC9 | PC10 | PC11 | PC12 | PC13 | PC14 | PC15 |
|---|---|---|---|---|---|---|---|---|---|---|---|---|---|---|---|---|
| **L10** | x10 | -0.08745 | 0.021019 | 0.091563 | -0.03402 | 0.207586 | 0.029018 | -0.02845 | -0.08795 | -0.00265 | 0.223047 | -0.00081 | -0.02857 | 0.139242 | -0.00539 | -0.26756 |
| | y10 | -0.0538 | -0.01022 | -0.26926 | 0.197055 | 0.062142 | -0.13467 | -0.13574 | 0.062198 | 0.046889 | 0.364994 | 0.139976 | 0.266668 | 0.017042 | 0.025824 | 0.265062 |
| | z10 | 0.022832 | 0.190194 | 0.048055 | 0.150564 | 0.174309 | 0.041802 | -0.15861 | 0.094575 | 0.208055 | -0.11298 | -0.10992 | 0.064646 | 0.048291 | -0.15034 | -0.07608 |
| **L11** | x11 | -0.08745 | 0.021019 | 0.091563 | -0.03402 | 0.207586 | 0.029018 | -0.02845 | -0.08795 | -0.00265 | 0.223047 | -0.00081 | -0.02857 | 0.139242 | -0.00539 | -0.26756 |
| | y11 | 0.053801 | 0.010221 | 0.269259 | -0.19706 | -0.06214 | 0.134668 | 0.13574 | -0.0622 | -0.04689 | -0.36499 | -0.13998 | -0.26667 | -0.01704 | -0.02582 | -0.26506 |
| | z11 | 0.022832 | 0.190194 | 0.048055 | 0.150564 | 0.174309 | 0.041802 | -0.15861 | 0.094575 | 0.208055 | -0.11298 | -0.10992 | 0.064646 | 0.048291 | -0.15034 | -0.07608 |
| **L12** | x12 | 0.184719 | -0.3211 | -0.02118 | -0.1431 | -0.07756 | 0.027358 | -0.15959 | 0.100145 | 0.148558 | 0.026207 | 0.030104 | -0.10337 | 0.00059 | -0.04809 | 0.098267 |
| | y12 | -0.03703 | 0.037937 | -2E-06 | 0.111237 | -0.05852 | 0.064741 | -0.29342 | -0.22376 | -0.01261 | 0.044347 | -0.18258 | 0.020654 | -0.15664 | -0.16644 | -0.10327 |
| | z12 | 0.031832 | -0.06925 | -0.08752 | 0.068456 | -0.11947 | 0.177778 | 0.059362 | -0.28649 | -0.06335 | -0.04444 | -0.03032 | 0.128682 | 0.169205 | 0.132236 | 0.118214 |
| **L13** | x13 | 0.184719 | -0.3211 | -0.02118 | -0.1431 | -0.07756 | 0.027358 | -0.15959 | 0.100145 | 0.148558 | 0.026207 | 0.030104 | -0.10337 | 0.00059 | -0.04809 | 0.098267 |
| | y13 | 0.037034 | -0.03794 | 0.000002 | -0.11124 | 0.058523 | -0.06474 | 0.293419 | 0.223757 | 0.012605 | -0.04435 | 0.18258 | -0.02065 | 0.156639 | 0.166438 | 0.103272 |
| | z13 | 0.031832 | -0.06925 | -0.08752 | 0.068456 | -0.11947 | 0.177778 | 0.059362 | -0.28649 | -0.06335 | -0.04444 | -0.03032 | 0.128682 | 0.169205 | 0.132236 | 0.118214 |
| **L14** | x14 | 0.260513 | -0.31805 | -0.127 | -0.13795 | -0.09031 | -0.06183 | -0.16196 | 0.006884 | 0.183675 | 0.030991 | 0.064284 | 0.153929 | 0.060274 | 0.055851 | -0.26852 |
| | y14 | 0 | 0 | 0 | 0 | 0 | 0 | 0 | 0 | 0 | 0 | 0 | 0 | 0 | 0 | 0 |
| | z14 | -0.00748 | -0.14291 | -0.00758 | -0.03579 | -0.06224 | 0.163912 | 0.052069 | 0.097527 | -0.01617 | 0.004651 | 0.003413 | 0.082428 | 0.218477 | -0.26036 | 0.065194 |
| **L15** | x15 | 0.006544 | 0.153855 | -0.26292 | -0.00726 | 0.095039 | -0.27452 | 0.300366 | -0.15358 | 0.147331 | -0.12788 | -0.21227 | 0.118217 | 0.156192 | -0.05012 | 0.063296 |
| | y15 | 0 | 0 | 0 | 0 | 0 | 0 | 0 | 0 | 0 | 0 | 0 | 0 | 0 | 0 | 0 |
| | z15 | -0.02544 | 0.124091 | -0.17039 | -0.13477 | -0.01898 | -0.07986 | -0.24429 | 0.113158 | -0.54476 | -0.19684 | 0.219965 | -0.00418 | 0.236639 | 0.212957 | -0.08283 |
| **L16** | x16 | 0.031806 | -0.06684 | -0.09362 | 0.005825 | -0.05853 | -0.16224 | -0.15391 | -0.14479 | -0.0527 | -0.11368 | -0.30385 | -0.03032 | 0.069602 | 0.060143 | 0.036119 |
| | y16 | 0 | 0 | 0 | 0 | 0 | 0 | 0 | 0 | 0 | 0 | 0 | 0 | 0 | 0 | 0 |
| | z16 | 0.035554 | 0.191868 | -0.15188 | -0.11361 | -0.0522 | 0.192756 | 0.076167 | 0.226154 | 0.188224 | -0.09746 | 0.079262 | -0.07957 | 0.201747 | 0.033657 | -0.08297 |
| **L17** | x17 | -0.2237 | -0.10117 | -0.08888 | 0.101602 | -0.03939 | 0.050937 | 0.115812 | -0.03119 | -0.15654 | -0.12726 | 0.052981 | 0.065044 | 0.019271 | -0.3155 | 0.115812 |
| | y17 | -0.26857 | -0.06543 | -0.12874 | -0.00497 | -0.24699 | 0.065309 | 0.050174 | -0.00423 | 0.094693 | -0.08148 | 0.181516 | 0.059703 | -0.16928 | -0.10133 | -0.16494 |
| | z17 | 0.369186 | 0.068821 | 0.051164 | 0.069442 | -0.07157 | 0.030455 | 0.209342 | -0.00767 | -0.10754 | 0.17545 | -0.0084 | 0.011674 | -0.27469 | -0.14139 | 0.04194 |
| **L18** | x18 | -0.2237 | -0.10117 | -0.08888 | 0.101602 | -0.03939 | 0.050937 | 0.115812 | -0.03119 | -0.15654 | -0.12726 | 0.052981 | 0.065044 | 0.019271 | -0.3155 | 0.115812 |
| | y18 | 0.268568 | 0.065426 | 0.128738 | 0.004965 | 0.24699 | -0.06531 | -0.05017 | 0.004225 | -0.09469 | 0.081483 | -0.18152 | -0.0597 | 0.169281 | 0.101331 | 0.164943 |
| | z18 | 0.369186 | 0.068821 | 0.051164 | 0.069442 | -0.07157 | 0.030455 | 0.209342 | -0.00767 | -0.10754 | 0.17545 | -0.0084 | 0.011674 | -0.27469 | -0.14139 | 0.04194 |

**Table B.1 (cont.): Male African cohort – Principal component scores (eigenvectors) using the symmetrical covariance matrix**

| | | PC1 | PC2 | PC3 | PC4 | PC5 | PC6 | PC7 | PC8 | PC9 | PC10 | PC11 |
|---|---|---|---|---|---|---|---|---|---|---|---|---|
| **L1** | x1 | -0.02455 | -0.10227 | 0.197335 | -0.00715 | -0.05192 | -0.13807 | 0.372496 | 0.026487 | -0.07438 | 0.126548 | 0.216129 |
| | y1 | 0 | 0 | 0 | 0 | 0 | 0 | 0 | 0 | 0 | 0 | 0 |
| | z1 | 0.016751 | 0.087923 | -0.21869 | -0.34099 | 0.449293 | -0.18279 | -0.14884 | 0.156432 | 0.276679 | -0.23448 | 0.14237 |
| **L2** | x2 | 0.026716 | 0.251852 | 0.17953 | -0.36151 | -0.11087 | -0.08806 | -0.23747 | -0.28227 | 0.069386 | 0.130504 | -0.1549 |
| | y2 | 0 | 0 | 0 | 0 | 0 | 0 | 0 | 0 | 0 | 0 | 0 |
| | z2 | -0.07978 | -0.29315 | -0.39892 | -0.25931 | 0.111049 | 0.245786 | -0.16933 | -0.07465 | -0.38486 | -0.012 | -0.0004 |
| **L3** | x3 | -0.12253 | 0.152459 | -0.14577 | 0.079352 | -0.00631 | 0.146947 | -0.01401 | 0.152209 | -0.31614 | -0.13217 | -0.26532 |
| | y3 | 0 | 0 | 0 | 0 | 0 | 0 | 0 | 0 | 0 | 0 | 0 |
| | z3 | 0.313315 | -0.00615 | -0.19864 | 0.006751 | 0.121135 | 0.102667 | 0.152917 | -0.0278 | -0.0073 | 0.118112 | 0.213186 |
| **L4** | x4 | -0.31156 | -0.02409 | -0.08878 | 0.147639 | -0.04998 | -0.12249 | 0.065656 | -0.01286 | -0.17092 | 0.047328 | 0.293016 |
| | y4 | 0 | 0 | 0 | 0 | 0 | 0 | 0 | 0 | 0 | 0 | 0 |
| | z4 | 0.3926 | -0.0332 | -0.13217 | 0.357984 | -0.05723 | -0.42136 | -0.30921 | 0.025736 | -0.0138 | -0.26058 | 0.007882 |
| **L5** | x5 | 0.043035 | -0.13261 | 0.104907 | 0.048923 | 0.116662 | -0.1261 | 0.124345 | -0.0486 | 0.016368 | -0.07495 | 0.014704 |
| | y5 | 0.035825 | 0.210805 | -0.00216 | -0.19077 | -0.08849 | -0.29764 | 0.047142 | 0.30656 | -0.31513 | -0.02208 | -0.0214 |
| | z5 | 0.048658 | 0.17839 | -0.03045 | 0.158725 | -0.13525 | 0.024067 | -0.05247 | 0.046877 | 0.032466 | 0.135415 | 0.037131 |
| **L6** | x6 | 0.043035 | -0.13261 | 0.104907 | 0.048923 | 0.116662 | -0.1261 | 0.124345 | -0.0486 | 0.016368 | -0.07495 | 0.014704 |
| | y6 | -0.03583 | -0.21081 | 0.002161 | 0.190766 | 0.08849 | 0.297641 | -0.04714 | -0.30656 | 0.315131 | 0.02208 | 0.0214 |
| | z6 | 0.048658 | 0.17839 | -0.03045 | 0.158725 | -0.13525 | 0.024067 | -0.05247 | 0.046877 | 0.032466 | 0.135415 | 0.037131 |
| **L7** | x7 | -0.02593 | -0.18335 | -0.04922 | 0.156575 | 0.003809 | 0.049535 | -0.13665 | -0.01484 | -0.07345 | -0.00093 | -0.01079 |
| | y7 | 0.078703 | 0.37895 | -0.09352 | 0.150186 | -0.07545 | 0.310721 | 0.044638 | 0.049701 | 0.00381 | -0.08675 | 0.068527 |
| | z7 | 0.27689 | -0.05333 | 0.120576 | -0.04279 | -0.15904 | -0.06191 | 0.192151 | -0.20598 | -0.08435 | -0.04414 | -0.12588 |
| **L8** | x8 | -0.02593 | -0.18335 | -0.04922 | 0.156575 | 0.003809 | 0.049535 | -0.13665 | -0.01484 | -0.07345 | -0.00093 | -0.01079 |
| | y8 | -0.0787 | -0.37895 | 0.09352 | -0.15019 | 0.07545 | -0.31072 | -0.04464 | -0.0497 | -0.00381 | 0.086752 | -0.06853 |
| | z8 | 0.27689 | -0.05333 | 0.120576 | -0.04279 | -0.15904 | -0.06191 | 0.192151 | -0.20598 | -0.08435 | -0.04414 | -0.12588 |
| **L9** | x9 | 0.170767 | 0.050636 | 0.174981 | -0.28889 | -0.20837 | 0.14958 | -0.23766 | 0.201183 | 0.186553 | -0.0024 | -0.13743 |
| | y9 | 0 | 0 | 0 | 0 | 0 | 0 | 0 | 0 | 0 | 0 | 0 |
| | z9 | -0.34567 | 0.359945 | 0.186106 | 0.151449 | 0.259384 | -0.13096 | -0.13581 | -0.35084 | 0.014373 | 0.02964 | 0.083478 |
| **L10** | x10 | 0.0184 | 0.132411 | 0.005073 | -0.07577 | 0.140145 | 0.021949 | -0.04419 | -0.03701 | -0.08366 | 0.094948 | -0.06951 |
| | y10 | 0.053963 | -0.04348 | -0.01742 | 0.121505 | -0.07635 | 0.10937 | -0.08406 | 0.019742 | 0.004736 | -0.11778 | -0.03746 |
| | z10 | -0.1225 | -0.14092 | 0.176825 | 0.133211 | 0.027953 | -0.00708 | -0.1519 | 0.320434 | 0.069305 | 0.256985 | -0.10891 |
| **L11** | x11 | 0.0184 | 0.132411 | 0.005073 | -0.07577 | 0.140145 | 0.021949 | -0.04419 | -0.03701 | -0.08366 | 0.094948 | -0.06951 |
| | y11 | -0.05396 | 0.043482 | 0.017418 | -0.12151 | 0.076351 | -0.10937 | 0.084061 | -0.01974 | -0.00474 | 0.117779 | 0.037455 |
| | z11 | -0.1225 | -0.14092 | 0.176825 | 0.133211 | 0.027953 | -0.00708 | -0.1519 | 0.320434 | 0.069305 | 0.256985 | -0.10891 |
| **L12** | x12 | 0.105802 | 0.010646 | -0.1201 | -0.00058 | 0.066708 | 0.03382 | 0.131745 | 0.025771 | 0.209764 | 0.171634 | -0.02037 |
| | y12 | -0.01487 | -0.00392 | -0.03672 | 0.017224 | 0.045691 | -0.01814 | 0.067512 | -0.1732 | 0.055958 | -0.16712 | -0.24842 |
| | z12 | -0.15938 | -0.12348 | -0.00347 | -0.19228 | -0.31511 | 0.09337 | -0.04942 | -0.08588 | 0.01399 | -0.07464 | 0.071654 |
| **L13** | x13 | 0.105802 | 0.010646 | -0.1201 | -0.00058 | 0.066708 | 0.03382 | 0.131745 | 0.025771 | 0.209764 | 0.171634 | -0.02037 |
| | y13 | 0.014866 | 0.003916 | 0.036719 | -0.01722 | -0.04569 | 0.018142 | -0.06751 | 0.1732 | -0.05596 | 0.167121 | 0.248423 |
| | z13 | -0.15938 | -0.12348 | -0.00347 | -0.19228 | -0.31511 | 0.09337 | -0.04942 | -0.08588 | 0.01399 | -0.07464 | 0.071654 |
| **L14** | x14 | 0.103432 | -0.01694 | -0.19568 | -0.00197 | -0.00297 | 0.078131 | 0.099202 | 0.159957 | 0.210745 | 0.017437 | 0.020671 |
| | y14 | 0 | 0 | 0 | 0 | 0 | 0 | 0 | 0 | 0 | 0 | 0 |
| | z14 | -0.20385 | 0.055598 | 0.012698 | -0.10781 | -0.12732 | 0.026964 | 0.36885 | 0.203709 | 0.187971 | -0.31443 | 0.220688 |
| **L15** | x15 | -0.05159 | 0.036741 | 0.168491 | 0.142137 | 0.00279 | 0.051187 | 0.030904 | 0.027847 | -0.23385 | -0.28845 | -0.01923 |
| | y15 | 0 | 0 | 0 | 0 | 0 | 0 | 0 | 0 | 0 | 0 | 0 |
| | z15 | -0.01738 | 0.107784 | -0.27591 | 0.00569 | -0.02361 | -0.09768 | 0.115298 | -0.20389 | -0.14166 | 0.399103 | 0.017476 |
| **L16** | x16 | 0.065939 | -0.00404 | -0.03571 | 0.005115 | -0.06214 | 0.068915 | 0.048886 | 0.020819 | 0.003458 | 0.074764 | -0.08319 |
| | y16 | 0 | 0 | 0 | 0 | 0 | 0 | 0 | 0 | 0 | 0 | 0 |
| | z16 | -0.26521 | 0.010251 | -0.14088 | 0.075413 | 0.098896 | -0.0489 | 0.282442 | 0.076152 | 0.135302 | -0.11586 | -0.59105 |
| **L17** | x17 | -0.06962 | 0.000729 | -0.06786 | 0.013487 | -0.08244 | -0.05228 | -0.13925 | -0.07201 | 0.093549 | -0.17749 | 0.151094 |
| | y17 | -0.15165 | 0.029136 | -0.10665 | 0.064482 | -0.25991 | -0.1389 | -0.05012 | -0.03147 | 0.169194 | 0.030108 | -0.02243 |
| | z17 | 0.050949 | -0.00517 | 0.319727 | -0.00146 | 0.165642 | 0.204684 | -0.01652 | 0.022121 | -0.06477 | -0.07837 | 0.079183 |
| **L18** | x18 | -0.06962 | 0.000729 | -0.06786 | 0.013487 | -0.08244 | -0.05228 | -0.13925 | -0.07201 | 0.093549 | -0.17749 | 0.151094 |
| | y18 | 0.151647 | -0.02914 | 0.106647 | -0.06448 | 0.259909 | 0.138904 | 0.05012 | 0.031466 | -0.16919 | -0.03011 | 0.022434 |
| | z18 | 0.050949 | -0.00517 | 0.319727 | -0.00146 | 0.165642 | 0.204684 | -0.01652 | 0.022121 | -0.06477 | -0.07837 | 0.079183 |

**Table B.2: Male Caucasian cohort – Principal component scores (eigenvectors) using the symmetric covariance matrix**

| | African | Caucasian |
|---|---|---|
| Procrustes distance | 0.03293055 | 0.04719008 |
| Mahalanobis distance | 1.7950 | 1.8011 |
| T-square value | 13.6458 | 9.9809 |
| P-value | 0.9990 | 0.9949 |

**Table B.3: Discriminant function analysis outputs**

# Appendix C – PRTools Script for Feature Selection and Classification

Feature selection and classification script for the African control and schizophrenia cohorts

```
% IMPORTING DATA
MAdata = importdata('H:\Craniofacial Dysmorphology\Matlab\MA\PC Scores MA.txt');
% Imports data from selected file (xlsx, csv, txt)
PCscoresMA = MAdata.data;
% Selects cells containing raw data (no labels) and imports as a matrix
Id = MAdata.textdata(2:end,1);
% Select column with labels and imports as a column vector
Diag = MAdata.textdata(2:end,2);
% Selects classifier column (e.g. diagnosis) and imports as a column vector

% USING PRTOOLS
A = prdataset(PCscoresMA,Diag);
% Creates a dataset from which pattern recognition tools can be used

% FEATURE SET EVALUATION
% Six feature set evaluations to determine best feature criterion
inin = feateval(A,'in-in');
mahas = feateval(A,'maha-s');
maham = feateval(A,'maha-m');
eucls = feateval(A,'eucl-s');
euclm = feateval(A,'eucl-m');
NN = feateval(A,'NN');

Eval = [inin mahas maham eucls euclm NN];
% Arranges feature set evaluations into a single vector

Maxeval = max(Eval);
% Returns the maximum of Eval indicating which feature selection criterion to use

% Function carried out to assign which feature selection criterion to use
if Maxeval == inin
    Crit = 'in-in';
elseif Maxeval == mahas
    Crit = 'maha-s';
elseif Maxeval == maham
    Crit = 'maha-m';
elseif Maxeval == eucls
    Crit = 'eucl-s';
elseif Maxeval == euclm
    Crit = 'eucl-m';
else Maxeval = 'NN';
end

% FEATURE SELECTION
B = featselo(A,Crit);
% Branch-and-bound feature selection - default # features = 2
C = featselp(A,Crit,2);
% Floating feature selection - selects optimal subset, Default criterion = NN

% Leave-one-out cross-validation before feature selection
LOOAw1 = prcrossval(A,nmc);
LOOAw2 = prcrossval(A,loglc);
LOOAw3 = prcrossval(A,svc);
LOOAw4 = prcrossval(A,qdc);
LOOAw5 = prcrossval(A,knnc);
LOOA = {LOOAw1,LOOAw2,LOOAw3,LOOAw4,LOOAw5}

MeanLOOA = mean([LOOAw1,LOOAw2,LOOAw3,LOOAw4,LOOAw5])

% Leave-one-out cross-validation after feature selection

LOODw1 = prcrossval(D,nmc);
LOODw2 = prcrossval(D,loglc);
```

```
LOODw3 = prcrossval(D,svc);
LOODw4 = prcrossval(D,qdc);
LOODw5 = prcrossval(D,knnc);
LOOD = {LOODw1,LOODw2,LOODw3,LOODw4,LOODw5}

MeanLOOD = mean([LOODw1,LOODw2,LOODw3,LOODw4,LOODw5])
```

Feature selection and classification script for the Caucasian control and schizophrenia cohorts

```
% IMPORTING DATA
MWdata = importdata('H:\Craniofacial Dysmorphology\Matlab\MW\PC Scores MW.txt');
% Imports data from selected file (xlsx, csv, txt)
PCscoresMW = MWdata.data;
% Selects cells containing raw data (no labels) and imports as a matrix
Id = MWdata.textdata(2:end,1);
% Select column with labels and imports as a column vector
Diag = MWdata.textdata(2:end,2);
% Selects classifier column (e.g. diagnosis) and imports as a column vector

% USING PRTOOLS
A = prdataset(PCscoresMW,Diag);
% Creates a dataset from which pattern recognition tools can be used

% FEATURE SET EVALUATION
% Six feature set evaluations to determine best feature criterion
inin = feateval(A,'in-in');
mahas = feateval(A,'maha-s');
maham = feateval(A,'maha-m');
eucls = feateval(A,'eucl-s');
euclm = feateval(A,'eucl-m');
NN = feateval(A,'NN');

Eval = [inin mahas maham eucls euclm NN];
% Arranges feature set evaluations into a single vector

Maxeval = max(Eval);
% Returns the maximum of Eval indicating which feature selection criterion to use

% Function carried out to assign which feature selection criterion to use
if Maxeval == inin
    Crit = 'in-in';
elseif Maxeval == mahas
    Crit = 'maha-s';
elseif Maxeval == maham
    Crit = 'maha-m';
elseif Maxeval == eucls
    Crit = 'eucl-s';
elseif Maxeval == euclm
    Crit = 'eucl-m';
else Maxeval = 'NN';
end

% FEATURE SELECTION
B = featselo(A,Crit);
% Branch-and-bound feature selection - default # features = 2
C = featselp(A,Crit,2);
% Floating feature selection - Selects optimal subset, Default criterion = NN

% Leave-one-out cross-validation before feature selection
LOOAw1 = prcrossval(A,nmc);
LOOAw2 = prcrossval(A,loglc);
LOOAw3 = prcrossval(A,svc);
LOOAw4 = prcrossval(A,qdc);
LOOAw5 = prcrossval(A,knnc);
LOOA = {LOOAw1,LOOAw2,LOOAw3,LOOAw4,LOOAw5}
```

```
MeanLOOA = mean([LOOAw1,LOOAw2,LOOAw3,LOOAw4,LOOAw5])

% Leave-one-out cross-validation after feature selection

LOODw1 = prcrossval(D,nmc);
LOODw2 = prcrossval(D,loglc);
LOODw3 = prcrossval(D,svc);
LOODw4 = prcrossval(D,qdc);
LOODw5 = prcrossval(D,knnc);
LOOD = {LOODw1,LOODw2,LOODw3,LOODw4,LOODw5}

MeanLOOD = mean([LOODw1,LOODw2,LOODw3,LOODw4,LOODw5])
```